物性研究55－2(1990－11)

修士論文　(1989年度)

スピングラスの有効場理論*

東京大学 理学部　　羽田野 直道

1　序文

Edwards と Anderson がスピングラスの平均場理論[1]を提唱して以来、その本質の解明に向けて多くの理論的研究[2]がなされてきた。なかでも、スピンが他のあらゆるスピンと長距離相互作用している Sherrington-Kirkpatrick (SK) 模型[3]は、レプリカ対称性の破れを起こす Parisi 解[4]により、その性質が明らかにされた。しかし一方、より現実的な短距離相互作用の模型については、まだいくつかの根本的な問題が残されている。スピングラス転移の下臨界次元 d_l はいくつか、また、臨界指数は古典的な値からどれだけずれるか、は興味ある点の1つだ。繰り込み群の予想によれば上臨界次元は6[5]となる。したがって、ϵ-展開の方法は2次元や3次元の系の臨界指数を調べるのに適切とは言えない。このため、ほとんどの研究はモンテカルロ・シミュレーション[23-27,29,31-34]によってなされてきた。

最近、臨界現象に対する新たな方法論として、鈴木によりコヒーレント異常法 (CAM)[6-8,11]が提唱された。相転移に対して平均場近似を行うと、転移点における応答関数の発散は古典的な、つまりランダウ型の臨界指数に従い、真のフラクショナルな指数からずれてしまう。しかし近似が改善されて真の振舞いに近づくとともに、臨界指数のずれを反映して応答関数の発散の留数が増大する。近似を系統的に（コヒーレントに）改善していったとき（例えば扱うクラスターを大きくしたとき）の留数の増大のしかたをコヒーレント異常と呼び、その異常の指数から、つまり真の系への近づき方から真の臨界指数を知る方法が CAM である。そこで、スピングラスに対して系統的に改善できる近似法を構成することが重要になる。

我々はこの論文で、スピングラスに対する有効場近似の構成法を提唱する。第2節でクラスター有効場理論の定式化を行う。この理論に従えば、扱うクラスターを順次大きくすることによって、系統的に近似が改善されることが期待される。第2節で得られた表式は、既に鈴木[10-12]によって提唱されている超有効場理論によっても導出することができる。第3節では超有効場理論について大まかに述べた後、スピングラスの超有効場理論の、実レプリカ法[10]による定式化について説明する。第4節では小さいクラスターに対する具体的な計算例を挙げ、また、2次元正方格子および3次元立方格子上の $\pm J$ 模型について得られた、すべての数値結果を報告する。第5節ではまず CAM 理論について概観し、第4節で得られた結果に対して行った CAM 理論によるデータ解析の結果を述べる。臨界点と臨界指数の評価を行い、第6節で他の方法による結果[25-34]と比較しながら検討する。以上の計算に用いたいくつかの性質を Appendix として付した。

*日本語による部分は、読者の便宜のために、「物性研究」編集部の要請により付加しました。

2　スピングラスの有効場理論の定式化（抜粋）

2.1　有効ハミルトニアン

Edwards-Anderson 模型

$$\mathcal{H}_{\mathrm{EA}}\{J_{ij}\} \equiv -\sum_{<ij>} J_{ij}\sigma_i\sigma_j - \mu_{\mathrm{B}}H\sum_i \sigma_i \tag{2.1}$$

について、ある有限クラスターにおける有効ハミルトニアンを以下のように定義する（ここで各ボンド J_{ij} は、ある分布関数に従ってそれぞれ独立に確率分布している）。無限系のハミルトニアンに対する分配関数 $Z\{J_{ij}\}$ を、あるクラスター Ω（図 1）の外側のスピンについてのみトレースすることによって、有効ハミルトニアン $\mathcal{H}_{\mathrm{eff}}$ は

$$e^{-\beta\mathcal{H}_{\mathrm{eff}}\{J_{ij}\}} \equiv \text{const. } \mathrm{Tr}_{\bar{\Omega}}\, e^{-\beta\mathcal{H}_{\mathrm{EA}}\{J_{ij}\}} \tag{2.6}$$

と定義できる。このときクラスターの周辺部 $\partial\Omega$ のスピンには、クラスターの外側のボンド分布に依存して確率分布する有効場がかかっている。

2.2　1 体有効場近似

上で述べた有効場には一般に、多数のスピンにかかる多体の有効場が含まれている。これらをすべて扱うのは不可能なので、以下では 1 体の有効場 H_{eff} のみを取り出し、それを自己無撞着条件を課して決める。また、高温側では有効場の確率分布はほぼガウス分布であるという仮定をおく（図 2）。

自己無撞着条件は、Edwards-Anderson の秩序変数がクラスターの中心と周辺部で等しい、つまり

$$[\langle\sigma_0\rangle^2]_{\mathrm{av.}} = [\langle\sigma_i\rangle^2]_{\mathrm{av.}}, \qquad {}^\forall i \in \partial\Omega \tag{2.15}$$

とおけばよい。上で述べた仮定などを用いれば、高温側では両辺の秩序変数を磁場 H および H_{eff} について展開することができて、

$$\sum_{j\in\partial\Omega} \alpha_{ij}[H_{\mathrm{eff}}(j)^2]_{\mathrm{av.}} = H^2\beta_i + O(H^4), \qquad {}^\forall i \in \partial\Omega \tag{2.25}$$

となる。ただし、行列 (α) とベクトル (β) は

$$\alpha_{ij} \equiv [\langle\sigma_i\sigma_j\rangle^2_{\Omega 0}]_{\mathrm{av.}} - [\langle\sigma_0\sigma_j\rangle^2_{\Omega 0}]_{\mathrm{av.}}, \tag{2.26}$$

$$\beta_i \equiv \sum_{J\in\Omega}\{[\langle\sigma_0\sigma_J\rangle^2_{\Omega 0}]_{\mathrm{av.}} - [\langle\sigma_i\sigma_J\rangle^2_{\Omega 0}]_{\mathrm{av.}}\}. \tag{2.27}$$

と定義されている。転移点 T_{SG} は、無限小の磁場 H に対して有限の有効場分布 $[H^2_{\mathrm{eff}}]_{\mathrm{av.}}$ が発生する点として

$$\det\alpha \equiv \det\left|[\langle\sigma_i\sigma_j\rangle^2_{\Omega 0}]_{\mathrm{av.}} - [\langle\sigma_0\sigma_j\rangle^2_{\Omega 0}]_{\mathrm{av.}}\right| = 0 \tag{2.32}$$

から求めることができる。スピングラス帯磁率は、この転移点近傍 $T \to T_{\mathrm{SG}} + 0$ で

$$\chi_{\mathrm{SG}} \simeq \overline{\chi}_{\mathrm{SG}} \cdot \frac{T_{\mathrm{SG}}}{T - T_{\mathrm{SG}}} \tag{2.33}$$

という形の古典的な発散を示す。

3 超有効場理論（SEFT）とスピングラスへの応用（抜粋）

3.1 SEFT の一般的な定式化

相転移の低温側では、系は対称性を破るような形の無限小の揺動に対して不安定になっている（図 3）。平均場理論では、平均場がその揺動の役割を果たしている。従来の平均場理論では、ハミルトニアンの変形によって平均場を導きだそうとしたため、限界があった。超有効場理論では、系の不安定性を調べるための自由度として *ad hoc* に場を導入する。ある秩序変数 $\langle Q\rangle \neq 0$ によって特徴づけられる相転移を調べるには、元の対称的なハミルトニアン $\mathcal{H}^{(0)}$ に対称性を破る項をつけ加えて、

$$\tilde{\mathcal{H}} \equiv \mathcal{H}^{(0)} - \Lambda Q \tag{3.3}$$

というハミルトニアンを定義する。秩序変数 Q は非局所的なもの（カイラルオーダーなど[12]）でもかまわない。

無限系のままでは扱えないので、有限のクラスター Ω に場 Λ と「超有効場」 $\Lambda_{\rm eff}$ をかけて[10-11]（図 4）、自己無撞着条件

$$\langle Q_0\rangle = \langle \tilde{Q}_i\rangle, \qquad {}^\forall i \in \partial\Omega, \tag{3.5}$$

を課す。両辺の秩序変数は、高温側では Λ と $\Lambda_{\rm eff}$ で展開できて、

$$\sum_{j\in\partial\Omega} \alpha_{ij}\Lambda_j = \Lambda\beta_i + O(\Lambda^2), \qquad {}^\forall i \in \partial\Omega \tag{3.11}$$

の形の式を得る。無限小の場 Λ に対して系が不安定になり、有限の超有効場 Λ_j が発生する点が転移点だと解釈できる。つまり[10-11]

$$\det\alpha \equiv \det\left|\langle \tilde{Q}_i\tilde{Q}_j\rangle_{\Omega 0} - \langle Q_0\tilde{Q}_j\rangle_{\Omega 0}\right| = 0 \tag{3.18}$$

から転移点 T_c が求められる。Q に対する応答関数も定義できて、$T \to T_c$ で古典的な発散を示す。

3.2 SEFT のスピングラスへの応用

スピングラスに応用する際には、ボンド分布はまったく同じ 2 つのクラスター（実レプリカ[10]）を用意して（図 5）、新しい秩序変数

$$Q \equiv \sum_i Q_i \equiv \sum_i \sigma_i^{(1)}\sigma_i^{(2)} \tag{3.22}$$

を導入する。これと共役な場 Λ は、2 つのレプリカ (1) と (2) にまたがる相互作用になる。$\Lambda = 0$ のときには

$$[\langle\sigma_i^{(1)}\sigma_i^{(2)}\rangle\big|_{\Lambda=0}]_{\rm av.} \equiv [\langle\sigma_i^{(1)}\rangle\langle\sigma_i^{(2)}\rangle\big|_{\Lambda=0}]_{\rm av.} \equiv [\langle\sigma_i\rangle^2]_{\rm av.} \tag{3.24}$$

となるので、Edwards-Anderson 秩序変数と同一になる。以下、上で述べた一般論にしたがえば、第 2 節で得た表式とまったく同じものを導くことができる[10-11]。

4　いくつかのクラスターにおける計算例と数値結果（抜粋）

以下の計算はすべて2次元正方格子と3次元立方格子上の $\pm J$ 模型で行った。すなわちスピンはイジングスピンとし、ボンドは等確率で $+J$ と $-J$ の値をとるものとする（図6）。

図7のクラスター（中心スピンと最近接スピンのみ）を用いた結果は、桂らによって既に得られているベーテ格子上のスピングラスの結果[20-21]と完全に一致する。さらに、隣接スピンの個数を無限大にする極限[9-10]をとると（図8）、Edwards-Anderson の平均場理論の結果[1]、つまりSK 模型の解[3]を得る。

さらに大きいクラスターについてはそれぞれ図13と図14に、得られた数値結果は表1と表2に列挙した。

5　コヒーレント異常法（CAM）による解析（抜粋）

5.1　CAM 理論

一般に2次相転移点 $T_c^{(*)}$ の近傍 $T \to T_c^{(*)} + 0$ では、秩序変数の応答関数が

$$\chi^{(*)}(T) \simeq \frac{C}{(T - T_c^{(*)})^{\gamma}} \tag{5.1}$$

の形で発散し、その発散の指数は上臨界次元より下で $\gamma > 1$ となっている。一方、第2節や第3節で述べた有効場型の近似では、転移点近傍 $T \to T_c^{(n)} > T_c^{(*)}$ において、

$$\chi^{(n)} \simeq \overline{\chi}^{(n)} \cdot \frac{T_c^{(n)}}{T - T_c^{(n)}} \tag{5.3}$$

という形の発散（$\gamma = 1$）しか示さない。しかしながら、近似を改善して $T_c^{(n)}$ と $\chi^{(n)}$ を真のものに近づければ、式 (5.1) と式 (5.3) の発散の指数の違いのために、式 (5.3) の係数 $\overline{\chi}^{(n)}$ が

$$\chi^{(n)} \simeq \frac{C'}{(T_c^{(n)} - T_c^{(*)})^{\psi}} \cdot \frac{T_c^{(n)}}{T - T_c^{(n)}} \tag{5.10}$$

という振舞いを示すことが期待される[6-7]。この振舞いをコヒーレント異常と呼ぶ。このとき、有限サイズ・スケーリング[22]あるいは有限近似度スケーリング[6-7]を用いて、コヒーレント異常関係式[6-7]

$$\gamma = \psi + 1 \tag{5.11}$$

を導くことができる。

この議論に従えば、ある系統的な近似列を構成して、それによって求められる $T_c^{(1)}, T_c^{(2)}, T_c^{(3)}, \cdots$, と $\overline{\chi}^{(1)}, \overline{\chi}^{(2)}, \overline{\chi}^{(3)}, \cdots$ を、関数 $\overline{\chi}^{(n)} = C'(T_c^{(n)} - T_c^{(*)})^{-\psi}$ にフィットすることによって、真の臨界点 $T_c^{(*)}$ と臨界指数 $\gamma = \psi + 1$ を精度よく評価することができる。

5.2　データ解析

上の一般論に従い、第4節で得られた数値結果を CAM 解析した。データ点の選び方を変えて、さまざまなフィットをした。結果は表3と表4に与えた。また、フィットの例を図15-19に挙げた。

6 結論とまとめ（抜粋）

6.1 2次元系に対する結論

2次元系においては、$T_{\rm SG}^{(*)} \equiv 0$ と仮定すると直線性のよいフィットができて（図 15）、臨界指数は

$$\gamma_s \simeq 5 \tag{6.4}$$

を得た。これは、表 5 に列挙した近年の研究の結果[23-31]とよい一致を示している。

6.2 3次元系に対する結論

3次元系においては、$T_{\rm SG}^{(*)} \sim 1.3(J_0/k_{\rm B})$ を得たが、データがばらついているために評価の誤差は大きく、臨界指数については確実な値を得ることができなかった。これは、扱ったクラスターの大きさが十分ではなかったためと思われる。

6.3 まとめ

スピングラスに対して有効場理論を構成し、平均場理論とベーテ格子に対する結果を再現した。さらに大きいクラスターでの計算によって、CAM 理論の応用が有用であることがわかった。特に2次元系ではゼロ点転移を確認し、そこでの臨界指数を精度よく評価できた。この結果は、他の研究によるものとよい一致を示している。ただし3次元系に関しては、さらに大きなクラスターでの計算が必要とされる。

A ゲージ対称性（抜粋）

相関関数のゲージ不変性[13-14]を用いて、

$$[\langle\sigma_{k_0}\sigma_{k_1}\rangle\langle\sigma_{k_1}\sigma_{k_2}\rangle\cdots\langle\sigma_{k_{n-2}}\sigma_{k_{n-1}}\rangle\langle\sigma_{k_{n-1}}\sigma_{k_n}\rangle]_{\rm av.} = 0, \qquad k_0 \neq k_n \tag{A.16}$$

という恒等式が示せる（図 22）。

B 分解定理（抜粋）

図 23 のように1点 j で接している2つのクラスター Ω_A と Ω_B にまたがる相関関数について、次のような分解定理を証明することができる。

定理 4（分解定理） Ω_A と Ω_B 上のイジング・スピングラス系において、それぞれスピン演算子 Q と R を考える。ある温度で $|\langle Q\rangle| \leq 1$ と $|\langle R\rangle| \leq 1$ が成り立っているものとする。このときその温度では

$$[\langle Q\rangle_A^2]_{\rm av.} = [\langle R\rangle_B^2]_{\rm av.} = [\langle\sigma_j\rangle_A^2]_{\rm av.} = [\langle\sigma_j\rangle_A^2]_{\rm av.} = 0 \implies$$
$$[\langle QR\rangle_{\rm tot}^n]_{\rm av.} = [\langle Q\sigma_j\rangle_A^n]_{\rm av.}[\langle\sigma_j R\rangle_B^n]_{\rm av.}, \qquad {}^\forall n \in N. \tag{B.22}$$

Master Thesis: Effective-Field Theory of Spin Glasses

Naomichi HATANO
Department of Physics, Faculty of Science, University of Tokyo

1 Introduction

Since Edwards and Anderson[1] proposed a mean-field theory, many theoretical studies[2] of spin glasses have been made. Among others, the Sherrington-Kirkpatrick model[3], which is a model with infinite-range interactions, is well explained by Parisi's solution[4] of the replica symmetry breaking. On the other hand, as concerns a more realistic model, not all the properties of the short-range Edwards-Anderson model[1] have been clarified yet. Non-classical critical-exponents of the spin-glass transition of the model is one of the most interesting problems. Since applications of the renormalization-group technique to the spin-glass transition have a difficulty: because the upper critical dimensionality is $d_u = 6$[5], we cannot rely on the ϵ-expansion to know the exponents of the 2- and 3- dimensional systems. For this reason, numerical-simulation approaches[23-27,29,31-34] have been made mainly.

Recently, a new approach to critical phenomena, the Coherent-Anomaly Method (CAM)[6-8,11], was proposed by Suzuki. Usually, an approximation of a mean-field type yields a singularity of the response-function with the classical, or Landau-type exponent, but the residue of it grows larger as the singularity point of the mean-field theory approaches the true critical point of the infinite system by an improvement of the approximation, reflecting the discrepancy between the classical exponent and the non-classical one. The CAM is the method for obtaining the non-classical critical exponents from a "coherent-anomaly", or the way of the residue to grow as the approximation is improved systematically, for example, as the treated cluster is enlarged. So it becomes important to construct a systematic series of approximations to the spin-glass transition.

In the present thesis, we construct a cluster-effective-field theory of spin glasses. In Section 2, formulae for the spin-glass transition point and the spin-glass susceptibility are obtained. They can improve in numerical values systematically in accord with enlargement of the cluster. In Section 3, it is mentioned

that these formulae agree with the results of Suzuki's Super-Effective-Field Theory (SEFT)[10-12]. Section 4 shows some examples of calculations, and also all the numerical results obtained are listed there. In Section 5, the critical exponents in the 2- and 3-dimensional systems are obtained from CAM-analyses. These results are discussed in Section 6, by comparing them with previous results by some other authors. Recent studies[25-34] of the critical exponents of the $\pm J$ model are listed there.

2 The Formulation of Effective-Field Theory of Spin Glasses

In the present section, an effective-field-approximation of the spin-glass transition is proposed. An expression for the spin-glass susceptibility in this approximation is obtained. The zero of the denominator of it gives the spin-glass transition point $T_{\rm SG}$.

2.1 Effective Hamiltonians

First, an effective Hamiltonian is defined for each sample. It contains effective-fields which themselves have their probability distributions.

Consider, as an original Hamiltonian, the short-range Edwards-Anderson model

$$\mathcal{H}_{\rm EA}\{J_{ij}\} \equiv -\sum_{<ij>} J_{ij}\sigma_i\sigma_j - \mu_{\rm B}H\sum_i \sigma_i, \tag{2.1}$$

where σ's denote Ising spins. Each interaction J_{ij} has its probability distribution $P(J_{ij})$ over samples. The free energy of the total system is defined as follows:

$$F \equiv [\log Z\{J_{ij}\}]_{\rm av.}, \tag{2.2}$$

where $Z\{J_{ij}\}$ denotes the partition function of a system of a bond configuration $\{J_{ij}\}$:

$$Z\{J_{ij}\} \equiv {\rm Tr}\ e^{-\beta\mathcal{H}_{\rm EA}\{J_{ij}\}}, \tag{2.3}$$

$$\beta \equiv \frac{1}{k_{\rm B}T}, \tag{2.4}$$

and $[\cdots]_{\rm av.}$ denotes the quenched-average:

$$[\cdots]_{\rm av.} \equiv \int\cdots\prod_{<ij>} P(J_{ij})dJ_{ij}. \tag{2.5}$$

For a system of a given bond-configuration, an effective Hamiltonian of a relevant cluster Ω (Figure 1) is defined by

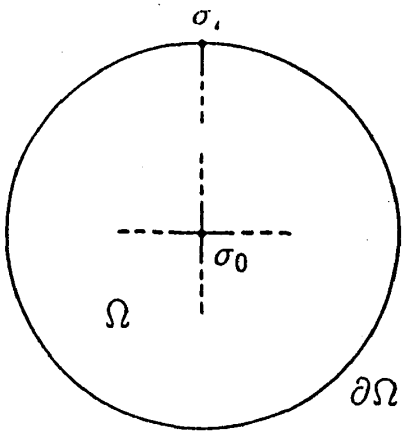

Figure 1: The cluster Ω.

$$e^{-\beta\mathcal{H}_{\rm eff}\{J_{ij}\}} \equiv \text{const. } \mathrm{Tr}_{\bar{\Omega}}\, e^{-\beta\mathcal{H}_{\rm EA}\{J_{ij}\}}, \tag{2.6}$$

where $\mathrm{Tr}_{\bar{\Omega}}$ denotes the trace with respect to spins which do *not* belong to the cluster Ω. This effective Hamiltonian can be written generally in the form

$$\begin{aligned}
\mathcal{H}_{\rm eff} &= \mathcal{H}_\Omega \\
&- \mu_{\rm B} \sum_{i\in\partial\Omega} H^{(1)}_{\rm eff}(i)\sigma_i \\
&- \mu_{\rm B} \sum_{i,j,k\in\partial\Omega} H^{(3)}_{\rm eff}(i,j,k)\sigma_i\sigma_j\sigma_k \\
&- \cdots \\
&- \sum_{i,j\in\partial\Omega} J^{(2)}_{\rm eff}(i,j)\sigma_i\sigma_j \\
&- \sum_{i,j,k,l\in\partial\Omega} J^{(4)}_{\rm eff}(i,j,k,l)\sigma_i\sigma_j\sigma_k\sigma_l \\
&- \cdots,
\end{aligned} \tag{2.7}$$

where

$$\mathcal{H}_\Omega \equiv -\sum_{<IJ>\in\Omega} J_{IJ}\sigma_I\sigma_J - \mu_{\rm B}H\sum_{I\in\Omega}\sigma_I \tag{2.8}$$

denotes the original Hamiltonian of the cluster Ω. Each of the effective-fields $H_{\rm eff}$, $J_{\rm eff}$ itself has its probability distribution due to the distributions of bonds of the outside of the cluster. Two lemmas can be proved.

Lemma 1 *Let the bond-distribution $P(J_{ij})$ be symmetric. In the paramagnetic phase with no magnetic fields, the quenched-averages of all the odd effective-fields vanish:*

$$[H^{(n)}_{\rm eff}]_{\rm av.} \equiv 0 \quad \textit{for } n = 1,3,5,\ldots \tag{2.9}$$

owing to the "gauge symmetry"[13-14].

Lemma 2 *Consider a spin operator S on the cluster Ω. In the paramagnetic phase, a quenched-average can be decomposed as follows:*

$$[\langle S\rangle_\Omega \cdot H_{\rm eff}^{(n)}]_{\rm av.} = [\langle S\rangle_\Omega]_{\rm av.} \cdot [H_{\rm eff}^{(n)}]_{\rm av.}, \tag{2.10}$$

where

$$\langle S\rangle_\Omega \equiv \frac{Tr_\Omega S e^{-\beta\mathcal{H}_\Omega}}{Tr_\Omega\ e^{-\beta\mathcal{H}_\Omega}}, \tag{2.11}$$

and Tr_Ω denotes the trace with respect to spins which belong to the cluster Ω, because the probability distributions of the bonds of the inside of the cluster and that of the outside of the cluster are independent with each other.

These lemmas are used in Section 2.2.

2.2 The One-Body-Effective-Field Approximation

Since it is impossible to determine the probability distributions of all the effective-fields, approximations must be introduced. In the present thesis, as an approximation, we neglect the "multi-body-effective-fields":

$$H_{\rm eff}^{(n)} \equiv 0 \quad \text{for} \quad n = 3, 5, 7, \ldots, \tag{2.12}$$

$$J_{\rm eff}^{(n)} \equiv 0 \quad \text{for} \quad n = 2, 4, 6, \ldots, \tag{2.13}$$

and determine the probability distributions of the "one-body-effective-fields $H_{\rm eff}^{(1)}(i)$" with a self-consistency condition. In the following, $H_{\rm eff}^{(1)}$ are abbreviated to $H_{\rm eff}$.

Let the bond-distribution be a symmetric function to use the gauge symmetry. An assumption must be made.

Assumption 3 *The probability distributions of the one-body-effective-fields in the paramagnetic phase can be assumed to follow nearly Gaussian distribution, i. e.*

$$[H_{\rm eff}^4]_{\rm av.} \sim [H_{\rm eff}^2]_{\rm av.}^2 \sim O(H^4). \tag{2.14}$$

On this assumption, it is sufficient to obtain the second moments of the probability distributions of the effective-fields for treating the paramagnetic phase. Then we make the self-consistency condition for the effective-fields as follows:

$$[\langle\sigma_0\rangle^2]_{\rm av.} = [\langle\sigma_i\rangle^2]_{\rm av.} \quad \text{for } {}^\forall i \in \partial\Omega, \tag{2.15}$$

where σ_0 denotes the spin at the centre of the cluster Ω. In the spin-glass phase, this assumption probably does not hold[15-19] and we will have to determine also higher moments. (Figure 2)

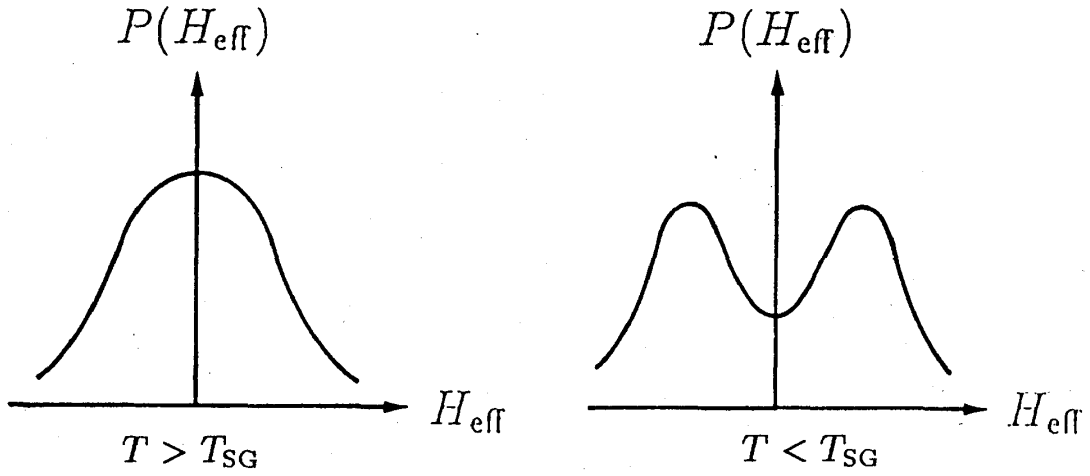

Figure 2: Schematic forms of the probability distribution of $H_{\rm eff}$.

To obtain an expression for the spin-glass susceptibility, we must discuss Equation (2.15) only of the order of H^2. For a given bond-configuration, we can expand in an applied magnetic field and effective-fields as follows:

$$\begin{aligned}\langle\sigma_0\rangle = \langle\sigma_0\rangle|_{H=H_{\rm eff}=0} &+ \sum_{J\in\Omega}\langle\sigma_0\sigma_J\rangle|_{H=H_{\rm eff}=0}\ K \\ &+ \sum_{j\in\partial\Omega}\langle\sigma_0\sigma_j\rangle|_{H=H_{\rm eff}=0}\ L_j \\ &+ O(K^2, KL, L^2),\end{aligned} \tag{2.16}$$

$$\begin{aligned}\langle\sigma_i\rangle = \langle\sigma_i\rangle|_{H=H_{\rm eff}=0} &+ \sum_{J\in\Omega}\langle\sigma_i\sigma_J\rangle|_{H=H_{\rm eff}=0}\ K \\ &+ \sum_{j\in\partial\Omega}\langle\sigma_i\sigma_j\rangle|_{H=H_{\rm eff}=0}\ L_j \\ &+ O(K^2, KL, L^2),\end{aligned} \tag{2.17}$$

where

$$K \equiv \beta\mu_{\rm B}H, \tag{2.18}$$

$$L_j \equiv \beta\mu_{\rm B}H_{\rm eff}(j). \tag{2.19}$$

Since multi-effective-fields are neglected, we can set

$$\langle\cdots\rangle|_{H=H_{\rm eff}=0} \equiv \langle\cdots\rangle_\Omega|_{H=0}. \tag{2.20}$$

These thermal-averages can be calculated analytically. Especially we obtain

$$\langle\sigma_0\rangle_\Omega|_{H=0} = \langle\sigma_i\rangle_\Omega|_{H=0} \equiv 0. \tag{2.21}$$

In the following, $\langle\cdots\rangle_\Omega|_{H=0}$ are abbreviated to $\langle\cdots\rangle_{\Omega 0}$. The expansion of $[\langle\sigma_0\rangle^2]_{\rm av.}$ gives

$$\begin{aligned}[\langle\sigma_0\rangle^2]_{\rm av.} &= \sum_{J\in\Omega}[\langle\sigma_0\sigma_J\rangle^2_{\Omega 0}]_{\rm av.}K^2 \\ &+ \sum_{I\neq J\in\Omega}[\langle\sigma_0\sigma_I\rangle_{\Omega 0}\langle\sigma_0\sigma_J\rangle_{\Omega 0}]_{\rm av.}K^2 \\ &+ \sum_{j\in\partial\Omega}[\langle\sigma_0\sigma_j\rangle^2_{\Omega 0}L_j^2]_{\rm av.} \\ &+ \sum_{i\neq j\in\partial\Omega}[\langle\sigma_0\sigma_i\rangle_{\Omega 0}\langle\sigma_0\sigma_j\rangle_{\Omega 0}L_iL_j]_{\rm av.} \\ &+ 2\sum_{J\in\Omega,j\in\partial\Omega}[\langle\sigma_0\sigma_J\rangle_{\Omega 0}\langle\sigma_0\sigma_j\rangle_{\Omega 0}L_j]_{\rm av.}K \\ &+ O(K^4)+O(K^2[L^2]_{\rm av.})+O([L^4]_{\rm av.}). \end{aligned} \tag{2.22}$$

The quenched-averages included in the third, fourth, and fifth terms can be decomposed owing to Lemma 2: (2.10). In addition to that, the second and fourth terms vanish owing to the gauge symmetry[13-14], (see Appendix A) and the fifth term vanishes owing to Lemma 1: (2.9). Terms $O(K^2[L^2]_{\rm av.})$ and $O([L^4]_{\rm av.})$ are of the order of K^4 owing to Assumption 3: (2.14). Also $[\langle\sigma_i\rangle^2]_{\rm av.}$ can be expanded similarly. Consequently, the remaining terms are

$$[\langle\sigma_0\rangle^2]_{\rm av.}=\sum_{J\in\Omega}[\langle\sigma_0\sigma_J\rangle^2_{\Omega 0}]_{\rm av.}K^2+\sum_{j\in\partial\Omega}[\langle\sigma_0\sigma_j\rangle^2_{\Omega 0}]_{\rm av.}[L_j^2]_{\rm av.}+O(K^4), \tag{2.23}$$

$$[\langle\sigma_i\rangle^2]_{\rm av.}=\sum_{J\in\Omega}[\langle\sigma_i\sigma_J\rangle^2_{\Omega 0}]_{\rm av.}K^2+\sum_{j\in\partial\Omega}[\langle\sigma_i\sigma_j\rangle^2_{\Omega 0}]_{\rm av.}[L_j^2]_{\rm av.}+O(K^4). \tag{2.24}$$

Substitution of (2.23) and (2.24) in the self-consistency condition (2.15) yields the set of the equations:

$$\sum_{j\in\partial\Omega}\alpha_{ij}[H_{\rm eff}(j)^2]_{\rm av.}=H^2\beta_i+O(H^4)\quad\text{for }{}^\forall i\in\partial\Omega, \tag{2.25}$$

where

$$\alpha_{ij}\equiv[\langle\sigma_i\sigma_j\rangle^2_{\Omega 0}]_{\rm av.}-[\langle\sigma_0\sigma_j\rangle^2_{\Omega 0}]_{\rm av.}, \tag{2.26}$$

$$\beta_i\equiv\sum_{J\in\Omega}\{[\langle\sigma_0\sigma_J\rangle^2_{\Omega 0}]_{\rm av.}-[\langle\sigma_i\sigma_J\rangle^2_{\Omega 0}]_{\rm av.}\}. \tag{2.27}$$

Equations (2.25) give the second moments of the effective-fields $H_{\rm eff}(j)$ in the form

$$\begin{aligned}[H_{\rm eff}(j)^2]_{\rm av.} &= H^2\sum_{i\in\partial\Omega}\alpha^{-1}_{ji}\beta_i+O(H^4) \\ &= \frac{H^2}{\det\alpha}\sum_{i\in\partial\Omega}\tilde\alpha_{ji}\beta_i+O(H^4), \end{aligned} \tag{2.28}$$

where the matrix $(\tilde{\alpha})$ denotes the cofactor matrix of the matrix (α):

$$(\alpha^{-1}) \equiv \frac{(\tilde{\alpha})}{\det \alpha}. \tag{2.29}$$

As previously mentioned, it is sufficient to determine the second moments of the probability distributions of the effective-fields for obtaining an expression for the spin-glass susceptibility in the paramagnetic phase. Substitution of (2.28) in (2.23) yields

$$\begin{aligned} [\langle\sigma_0\rangle^2]_{\rm av.} &= \{\sum_{J\in\Omega}[\langle\sigma_0\sigma_J\rangle^2_{\Omega 0}]_{\rm av.} \\ &+ \frac{1}{\det\alpha}\sum_{i,j\in\partial\Omega}[\langle\sigma_0\sigma_i\rangle^2_{\Omega 0}]_{\rm av.}\tilde{\alpha}_{ij}\beta_j\}K^2 + O(K^4). \end{aligned} \tag{2.30}$$

Then we arrive at the formula for the spin-glass susceptibility:

$$\begin{aligned} \chi_{\rm SG} &\equiv N\mu_{\rm B}^2 \frac{\partial}{\partial(H^2)}[\langle\sigma_0\rangle^2]_{\rm av.}\Big|_{H=0} \\ &= N\beta^2\mu_{\rm B}^4\{\sum_{J\in\Omega}[\langle\sigma_0\sigma_J\rangle^2_{\Omega 0}]_{\rm av.} \\ &\quad + \frac{1}{\det\alpha}\sum_{i,j\in\partial\Omega}[\langle\sigma_0\sigma_i\rangle^2_{\Omega 0}]_{\rm av.}\tilde{\alpha}_{ij}\beta_j\}. \end{aligned} \tag{2.31}$$

The spin-glass susceptibility diverges with the critical exponent $\gamma_{\rm s} = 1$. This divergence can be understood to correspond to the transition from the paramagnetic phase to the spin-glass phase. The spin-glass transition point $T_{\rm SG}$ is determined as follows:

$$\det\alpha \equiv \det\left|[\langle\sigma_i\sigma_j\rangle^2_{\Omega 0}]_{\rm av.} - [\langle\sigma_0\sigma_j\rangle^2_{\Omega 0}]_{\rm av.}\right| = 0 \quad \text{at } T = T_{\rm SG}. \tag{2.32}$$

Near and above the transition point, this spin-glass susceptibility of the type of the effective-field theory shows the following behaviour:

$$\chi_{\rm SG} \simeq \overline{\chi}_{\rm SG}\cdot\frac{T_{\rm SG}}{T - T_{\rm SG}} \qquad \text{as} \qquad T \to T_{\rm SG} + 0, \tag{2.33}$$

with

$$\overline{\chi}_{\rm SG} = \frac{N\mu_{\rm B}^4}{k_{\rm B}^2 T_{\rm SG}^3}\cdot\left.\frac{\sum_{i,j\in\partial\Omega}[\langle\sigma_0\sigma_i\rangle^2_{\Omega 0}]_{\rm av.}\tilde{\alpha}_{ij}\beta_j}{\frac{d}{dT}\det\alpha}\right|_{T=T_{\rm SG}} \tag{2.34}$$

This quantity (2.34) plays an important role in the CAM: See Section 5.

When all the $z_{\partial\Omega}$ sites $i \in \partial\Omega$ are located in equivalent positions in view of geometrical symmetries of the cluster Ω, we can set

$$\because [H_{\rm eff}^2(i)]_{\rm av.} \equiv [H_{\rm eff}^2]_{\rm av.}. \tag{2.35}$$

Then the expressions (2.31), (2.32) and (2.34) take the rather simple forms

$$C_0 = C_1 \quad \text{at} \quad T = T_{\rm SG}, \tag{2.36}$$

$$\chi_{\rm SG} = N\beta^2\mu_{\rm B}^4 \frac{C_0B_1 - C_1B_0}{C_0 - C_1}, \tag{2.37}$$

$$\overline{\chi}_{\rm SG} = \frac{N\mu_{\rm B}^4}{k_{\rm B}^2T_{\rm SG}^3} \cdot \left.\frac{(C_0B_1 - C_1B_0)}{\frac{d}{dT}(C_0 - C_1)}\right|_{T=T_{\rm SG}}, \tag{2.38}$$

respectively, where

$$B_0 \equiv \sum_{J\in\Omega}[\langle\sigma_0\sigma_J\rangle_{\Omega 0}^2]_{\rm av.}, \tag{2.39}$$

$$B_1 \equiv \sum_{J\in\Omega}[\langle\sigma_i\sigma_J\rangle_{\Omega 0}^2]_{\rm av.}, \tag{2.40}$$

$$C_0 \equiv \sum_{j\in\partial\Omega}[\langle\sigma_0\sigma_i\rangle_{\Omega 0}^2]_{\rm av.} = z_{\partial\Omega}[\langle\sigma_0\sigma_i\rangle_{\Omega 0}^2]_{\rm av.}, \tag{2.41}$$

and

$$C_1 \equiv \sum_{j\in\partial\Omega}[\langle\sigma_i\sigma_j\rangle_{\Omega 0}^2]_{\rm av.} = \sum_{j=1}^{z_{\partial\Omega}}[\langle\sigma_i\sigma_j\rangle_{\Omega 0}^2]_{\rm av.}. \tag{2.42}$$

for $^{\exists}i \in \partial\Omega$. It can be understood[10] that Equation (2.36) with (2.41) and (2.42) represents balance between "ordering effects" and "disordering effects".

These are the results of the one-body-effective-field approximation for the cluster Ω. It is expected that the approximation is improved gradually as we calculate on larger clusters.

3 The Super-Effective-Field-Theory (SEFT) and Its Application to Spin Glasses

The formulae obtained in the previous section agree with the results of the Super-Effective-Field Theory (SEFT)[10-12] proposed by Suzuki. In the present section, the general formulation of the SEFT and its application[10] to spin glasses are reviewed.

3.1 The General Formulation of the SEFT

A phase transition is none other than spontaneous symmetry breaking. In the low-temperature phase, an infinitesimal perturbation of a symmetry-breaking type causes instability and the whole system falls into a non-symmetric state: See Figure 3. In a usual effective-field theory, the effective-field plays a role of such a perturbation. It has been, however, always justified to introduce the effective-field by some modifications of the original Hamiltonian of the system. In the SEFT, the super-effective-field is introduced *ad hoc* as an extra degree of freedom to examine the stability of the system.

Consider a phase transition characterized by an order parameter $\langle Q \rangle \neq 0$, where Q is the sum of local or semi-local operators $\{Q_i\}$ with a modular factor ε_{0i}:

$$Q \equiv \sum_i \tilde{Q}_i, \tag{3.1}$$

where

$$\tilde{Q}_i \equiv \varepsilon_{0i} Q_i. \tag{3.2}$$

The operator Q_i is defined on a support S_i, which may be a site, a plaquette or something else. The modular factors[10-11] are introduced here to discuss, for example, staggered magnetization. A conjugate field Λ of the operator Q is applied on the original symmetric Hamiltonian $\mathcal{H}^{(0)}$ as follows:

$$\tilde{\mathcal{H}} \equiv \mathcal{H}^{(0)} - \Lambda Q. \tag{3.3}$$

It is expected that, because of instability, the limit operation $\Lambda \to 0$ after the thermodynamic limit yields $\langle Q \rangle \neq 0$ in the symmetry-breaking phase, and that the response of $\langle Q \rangle$ to Λ shows singular behaviour at the transition point.

Of course, for the system of this Hamiltonian cannot be solved exactly in most cases, we must make an approximation of it to the "super-effective" Hamiltonian[10-11] of the cluster Ω (Figure 4):

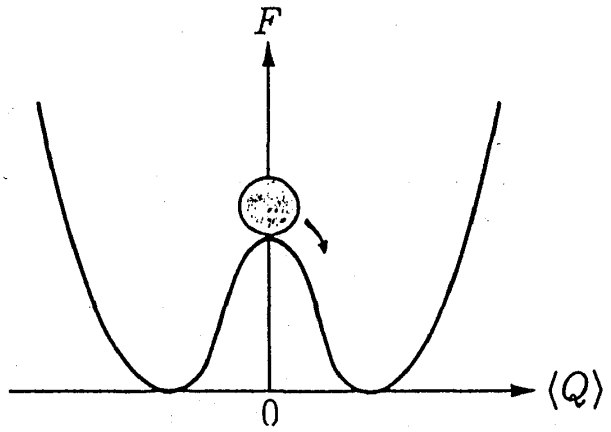

Figure 3: A "potential" of a system in its low-temperature phase.

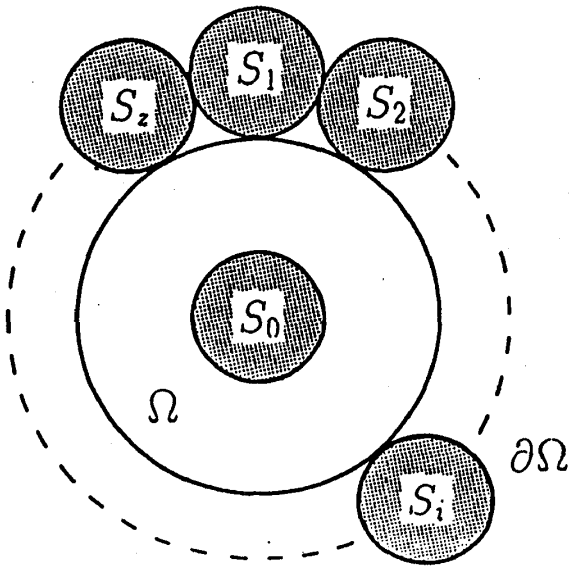

Figure 4: A cluster constructed of supports.

$$\tilde{\mathcal{H}}_s \equiv \mathcal{H}_\Omega^{(0)} - \Lambda \sum_{I\in\Omega} \tilde{Q}_I - \sum_{i\in\partial\Omega} \Lambda_i \tilde{Q}_i. \tag{3.4}$$

The "super-effective-fields" Λ_i are determined by the self-consistency conditions:

$$\langle Q_0 \rangle = \langle \tilde{Q}_i \rangle \quad \text{for } {}^\forall i \in \partial\Omega, \tag{3.5}$$

where Q_0 denotes the operator on the support S_0 at the centre of the cluster.

To obtain an expression for the response-function χ_Q, we have only to discuss quantities of the order of Λ. Expansions of $\langle Q_0 \rangle$ and $\langle \tilde{Q}_i \rangle$ in Λ and Λ_i give

$$\langle Q_0 \rangle = \sum_{J\in\Omega} \langle Q_0 \tilde{Q}_J \rangle_{\Omega 0}\, K + \sum_{j\in\partial\Omega} \langle Q_0 \tilde{Q}_j \rangle_{\Omega 0}\, \lambda_j + O(K^2, K\lambda, \lambda^2), \tag{3.6}$$

$$\langle \tilde{Q}_i \rangle = \sum_{J\in\Omega} \langle \tilde{Q}_i \tilde{Q}_J \rangle_{\Omega 0}\, K + \sum_{j\in\partial\Omega} \langle \tilde{Q}_i \tilde{Q}_j \rangle_{\Omega 0}\, \lambda_j + O(K^2, K\lambda, \lambda^2), \tag{3.7}$$

where

$$K \equiv \beta\Lambda, \tag{3.8}$$

$$\lambda_i \equiv \beta\Lambda_i, \tag{3.9}$$

and

$$\langle \cdots \rangle_{\Omega 0} \equiv \frac{\mathrm{Tr}_\Omega \cdots e^{-\beta\mathcal{H}_\Omega^{(0)}}}{\mathrm{Tr}_\Omega\, e^{-\beta\mathcal{H}_\Omega^{(0)}}}. \tag{3.10}$$

Substitution of (3.6) and (3.7) in (3.5) gives

$$\sum_{j\in\partial\Omega} \alpha_{ij}\Lambda_j = \Lambda\beta_i + O(\Lambda^2) \quad \text{for } {}^\forall i \in \partial\Omega, \tag{3.11}$$

where

$$\alpha_{ij} \equiv \langle \tilde{Q}_i \tilde{Q}_j \rangle_{\Omega 0} - \langle Q_0 \tilde{Q}_j \rangle_{\Omega 0}, \tag{3.12}$$

$$\beta_i \equiv \sum_{J \in \Omega} \{ \langle Q_0 \tilde{Q}_J \rangle_{\Omega 0} - \langle \tilde{Q}_i \tilde{Q}_J \rangle_{\Omega 0} \}. \tag{3.13}$$

The super-effective-fields are determined by

$$\Lambda_j = \frac{\Lambda}{\det \alpha} \sum_{i \in \partial\Omega} \tilde{\alpha}_{ji} \beta_i + O(\Lambda^2), \tag{3.14}$$

where we write

$$\alpha_{ij}^{-1} \equiv \frac{\tilde{\alpha}_{ij}}{\det \alpha}. \tag{3.15}$$

By substituting (3.14) in (3.6), $\langle Q_0 \rangle$ generated by Λ is written in the form

$$\begin{aligned} \langle Q_0 \rangle &= \{ \sum_{J \in \Omega} \langle Q_0 \tilde{Q}_J \rangle_{\Omega 0} \\ &+ \frac{1}{\det \alpha} \sum_{i,j \in \partial\Omega} \langle Q_0 \tilde{Q}_i \rangle_{\Omega 0} \tilde{\alpha}_{ij} \beta_j \} K + O(K^2). \end{aligned} \tag{3.16}$$

The expression for the response-function of the order parameter $\langle Q \rangle$ to Λ is, in this approximation, given[10-11] by

$$\begin{aligned} \chi_Q &\equiv N \frac{\partial}{\partial \Lambda} \langle Q_0 \rangle \Big|_{\Lambda=0} \\ &= N\beta \{ \sum_{J \in \Omega} \langle Q_0 \tilde{Q}_J \rangle_{\Omega 0} + \frac{1}{\det \alpha} \sum_{i,j \in \partial\Omega} \langle Q_0 \tilde{Q}_i \rangle_{\Omega 0} \tilde{\alpha}_{ij} \beta_j \}. \end{aligned} \tag{3.17}$$

The function (3.17) diverges at $\det \alpha = 0$. This divergence is expected to mean instability of the symmetric state and a transition to a symmetry-breaking phase. The transition point is determined by the following equation[10-11]:

$$\det \alpha \equiv \det \left| \langle \tilde{Q}_i \tilde{Q}_j \rangle_{\Omega 0} - \langle Q_0 \tilde{Q}_j \rangle_{\Omega 0} \right| = 0 \quad \text{at} \quad T = T_c. \tag{3.18}$$

At the transition point, the "susceptibility" (3.17) has a singularity with the classical exponent $\gamma = 1$ as follows:

$$\chi_Q \simeq \overline{\chi}_Q \cdot \frac{T_c}{T - T_c} \qquad \text{as} \quad T \to T_c + 0, \tag{3.19}$$

with[10-11]

$$\overline{\chi}_Q = \frac{N}{T_c^2} \cdot \left. \frac{\sum_{i,j \in \partial\Omega} \langle Q_0 \tilde{Q}_i \rangle_{\Omega 0} \tilde{\alpha}_{ij} \beta_j}{\frac{d}{dT} \det \alpha} \right|_{T=T_c}. \tag{3.20}$$

Formulation[10-11] for quantum systems are quite similar. The SEFT has been already applied to the chiral transition[12]: See the refernces of Ref.[11].

3.2 Applications of the SEFT to Spin Glasses

It is another problem how to apply the SEFT to spin glasses. In Suzuki's paper[10], two "real replicas" are introduced. The reason why the number of the replicas is two is that we need only the second moment of $\langle\sigma\rangle$.

The original Hamiltonian is given by

$$\mathcal{H}_0 \equiv -\sum_{\alpha=1,2}\sum_{<ij>} J_{ij}\sigma_i^{(\alpha)}\sigma_j^{(\alpha)}, \tag{3.21}$$

where α denotes each replica, and $\sigma^{(\alpha)}$ denotes a spin on the α-th replica. The bond-configurations of two replicas are the same as each other. The operator Q of (3.1) is defined as follows:

$$Q \equiv \sum_i Q_i \equiv \sum_i \sigma_i^{(1)}\sigma_i^{(2)}. \tag{3.22}$$

Then, corresponding to (3.3), the Hamiltonian which includes the conjugate field Λ is described[10] by

$$\tilde{\mathcal{H}} \equiv \mathcal{H}_0 - \Lambda\sum_i \sigma_i^{(1)}\sigma_i^{(2)}. \tag{3.23}$$

The field Λ is an interaction between two replicas. When $\Lambda = 0$, the two replicas decompose into two independent systems of the same bond-configuration, and we obtain the Edwards-Anderson order parameter from Q:

$$[\langle\sigma_i^{(1)}\sigma_i^{(2)}\rangle\big|_{\Lambda=0}]_{\text{av.}} \equiv [\langle\sigma_i^{(1)}\rangle\langle\sigma_i^{(2)}\rangle\big|_{\Lambda=0}]_{\text{av.}} \equiv [\langle\sigma_i\rangle^2]_{\text{av.}}. \tag{3.24}$$

The super-effective Hamiltonian for spin glasses is defined as follows (Figure 5):

$$\tilde{\mathcal{H}}_s \equiv \sum_{\alpha=1,2}\mathcal{H}_\Omega^{(\alpha)} - \Lambda\sum_{I\in\Omega}\sigma_I^{(1)}\sigma_I^{(2)}. - \sum_{i\in\partial\Omega}\Lambda_i\sigma_i^{(1)}\sigma_i^{(2)}, \tag{3.25}$$

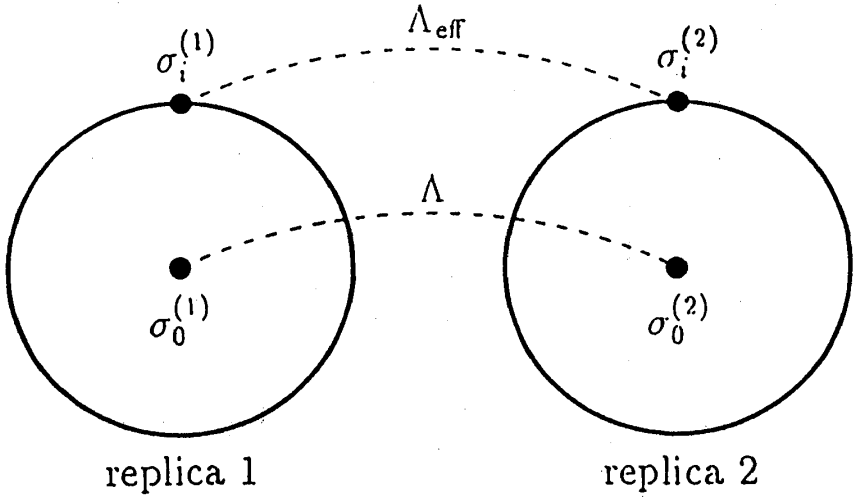

Figure 5: Two real replicas and super-effective fields between them.

where

$$\mathcal{H}_{\Omega}^{(\alpha)} \equiv -\sum_{<IJ>\in\Omega} J_{IJ}\sigma_I^{(\alpha)}\sigma_J^{(\alpha)}. \tag{3.26}$$

The self-consistency conditions for Λ_i are given by (3.5):

$$[\langle\sigma_0^{(1)}\sigma_0^{(2)}\rangle]_{\rm av.} = [\langle\sigma_i^{(1)}\sigma_i^{(2)}\rangle]_{\rm av.} \quad \text{for } {}^{\forall}i \in \partial\Omega. \tag{3.27}$$

The same calculations as (3.6) - (3.17) yield the response-function χ_Q[10]:

$$\begin{aligned}\chi_Q &\equiv N\frac{\partial}{\partial\Lambda}[\langle\sigma_0^{(1)}\sigma_0^{(2)}\rangle]_{\rm av.}\Big|_{\Lambda=0} \\ &= N\beta\{\sum_{J\in\Omega}[\langle\sigma_0\sigma_J\rangle_{\Omega 0}^2]_{\rm av.} + \frac{1}{\det\alpha}\sum_{i,j\in\partial\Omega}[\langle\sigma_0\sigma_i\rangle_{\Omega 0}^2]_{\rm av.}\tilde{\alpha}_{ij}\beta_j\}.\end{aligned} \tag{3.28}$$

This expression for the response-function agrees with that for the spin-glass susceptibility of the effective-field theory (2.31) in Section 2 except a factor. Also Equations (3.18) and (3.20) agree with (2.32) and (2.34) correspondingly.

4 Examples of Some Clusters and Numerical Results

In the following, we restrict ourselves to the $\pm J$ model, or the model with the following probability-distribution function of interactions (Figure 6):

$$P(J) \equiv \frac{1}{2}\{\delta(J - J_0) + \delta(J + J_0)\}, \tag{4.1}$$

with $J_0 > 0$. Examples of the effective-field approximation in Section 2 for two clusters and all the results obtained are mentioned in the present section.

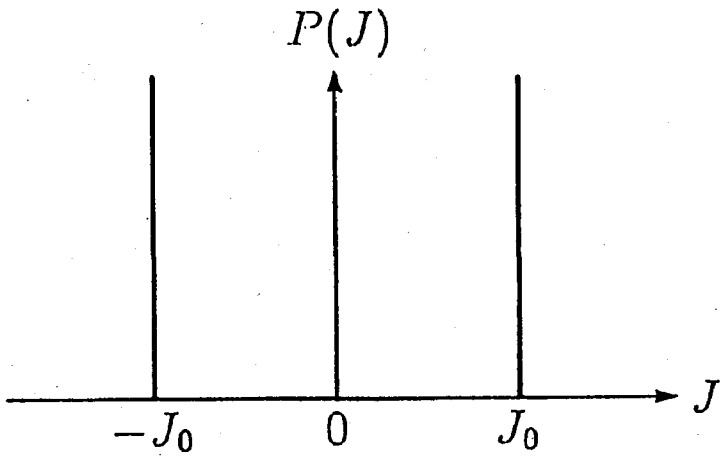

Figure 6: The $\pm J$ model.

4.1 The First Approximation (the "Bethe Approximation") and the Mean-Field Approximation as a Limit of It

First, consider[10] a site and the nearest-neighbouring sites of it as the cluster Ω: See Figure 7. This is the cluster used in the well-known Bethe approximation for the ferromagnetic phase transition. The Hamiltonian of this cluster is given by

$$\mathcal{H}_\Omega \equiv -\sum_{i=1}^{z} J_{0i}\sigma_0\sigma_i. \tag{4.2}$$

The correlation functions with respect to this Hamiltonian can be easily calculated as follows[10]:

$$\begin{aligned} \langle\sigma_0\sigma_i\rangle_{\Omega 0} &= \tanh\beta J_{0i} \\ &= A_{0i}t \quad \text{for } i = 1, 2, \cdots, z, \end{aligned} \tag{4.3}$$

$$\begin{aligned} \langle\sigma_i\sigma_j\rangle_{\Omega 0} &= \langle\sigma_i\sigma_0\rangle_{\Omega 0}\langle\sigma_0\sigma_j\rangle_{\Omega 0} \\ &= A_{i0}A_{0j}t^2 \quad \text{for } i \neq j \in \partial\Omega, \end{aligned} \tag{4.4}$$

where

$$A_{0i} \equiv \text{sgn } J_{0i}, \tag{4.5}$$

$$t \equiv \tanh\beta J_0 > 0. \tag{4.6}$$

Taking the quenched-averages of (4.3) and (4.4) with respect to the probability distribution (4.1) results in

$$[\langle\sigma_0\sigma_i\rangle_{\Omega 0}^2]_{\text{av.}} = t^2 \quad \text{for } {}^\forall i \in \partial\Omega, \tag{4.7}$$

$$[\langle\sigma_i\sigma_j\rangle_{\Omega 0}^2]_{\text{av.}} = t^4 \quad \text{for } {}^\forall i \neq j \in \partial\Omega. \tag{4.8}$$

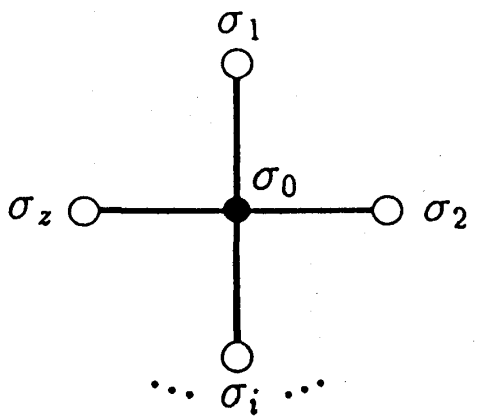

Figure 7: The cluster used in the "Bethe approximation". The symbol "o" denotes the boundary sites, at which the effective fields are applied.

The equation which determines the spin-glass transition point is (2.36), or

$$zt^2 = 1 + (z-1)t^4 \quad \text{at} \quad T = T_{\rm SG}, \tag{4.9}$$

which gives

$$\tanh\left(\frac{J_0}{k_{\rm B}T_{\rm SG}^{(\rm B)}}\right) = \frac{1}{\sqrt{z-1}}. \tag{4.10}$$

The spin-glass susceptibility is obtained from (2.37) in the form[10]

$$\chi_{\rm SG}^{(\rm B)} = N\beta^2\mu_{\rm B}^4 \frac{1+t^2}{1-(z-1)t^2}. \tag{4.11}$$

These expressions agree with that obtained by Katsura[20-21] using the method of the distribution function. Near the transition point, $\chi_{\rm SG}^{(\rm B)}$ behaves as (2.33) with

$$\overline{\chi}_{\rm SG}^{(\rm B)} = N\frac{\mu_{\rm B}^4}{J_0^2}\cdot\frac{J_0}{k_{\rm B}T_{\rm SG}^{(\rm B)}}\cdot\frac{z}{2(z-2)\sqrt{z-1}}. \tag{4.12}$$

The numerical results of (4.10) and (4.12) are as follows[10]: In the 2-dimensional system,

$$\left.\begin{aligned} &\tanh\left(\frac{J_0}{k_{\rm B}T_{\rm SG}^{(\rm B)}}\right) = \frac{1}{\sqrt{3}}, \\ &T_{\rm SG}^{(\rm B)} = 1.51865(J_0/k_{\rm B}), \\ &\overline{\chi}_{\rm SG}^{(\rm B)} = \frac{1}{\sqrt{3}\,T_{\rm SG}^{(\rm B)}} = 0.38017(\mu_{\rm B}^4/J_0^2), \end{aligned}\right\} \quad \text{for} \quad z = 4, \tag{4.13}$$

and in the 3-dimensional system,

$$\left.\begin{aligned} &\tanh\left(\frac{J_0}{k_{\rm B}T_{\rm SG}^{(\rm B)}}\right) = \frac{1}{\sqrt{5}}, \\ &T_{\rm SG}^{(\rm B)} = 2.07809(J_0/k_{\rm B}), \\ &\overline{\chi}_{\rm SG}^{(\rm B)} = \frac{3}{4\sqrt{5}\,T_{\rm SG}^{(\rm B)}} = 0.16140(\mu_{\rm B}^4/J_0^2), \end{aligned}\right\} \quad \text{for} \quad z = 6. \tag{4.14}$$

In the limit of $z \to \infty$, the asymptotic forms of (4.10) and (4.11) give[9-10]

$$T_{\rm SG}^{(\rm W)} \simeq \frac{J_0}{k_{\rm B}}\cdot\tanh^{-1}\left(\frac{J_0}{k_{\rm B}T_{\rm SG}^{(\rm W)}}\right) \simeq \frac{J_0}{k_{\rm B}}\cdot\sqrt{z}, \tag{4.15}$$

$$\chi_{\rm SG}^{(\rm W)} = N\beta^2\mu_{\rm B}^4\frac{1+K^2}{1-zK^2}, \tag{4.16}$$

$$\overline{\chi}_{\rm SG}^{(\rm W)} = N\frac{\mu_{\rm B}^4}{J_0^2}\cdot\frac{1}{2z}, \tag{4.17}$$

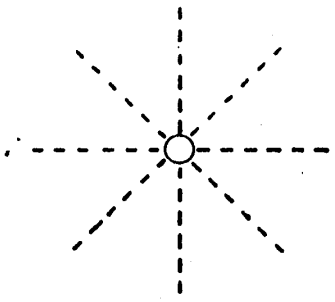

Figure 8: The "Weiss approximation", or the Sherrington-Kirkpatrick model.

where

$$K = \frac{J_0}{k_{\rm B}T}. \tag{4.18}$$

These expressions agree with that obtained from the mean-field theory by Edwards and Anderson[1], which correspond to the Weiss approximation of the ferromagnetic transition (Figure 8), or the solution of the Sherrington-Kirkpatrick model[3]. The numerical results of (4.15) and (4.17) are as follows: In the 2-dimensional system, we have

$$\left.\begin{aligned} T_{\rm SG}^{\rm (W)} &= 2(J_0/k_{\rm B}), \\ \overline{\chi}_{\rm SG}^{\rm (W)} &= \frac{1}{8}(\mu_{\rm B}^4/J_0^2), \end{aligned}\right\} \quad \text{for} \quad z = 4, \tag{4.19}$$

and in the 3-dimensional system, we obtain

$$\left.\begin{aligned} T_{\rm SG}^{\rm (W)} &= \sqrt{6}(J_0/k_{\rm B}), \\ \overline{\chi}_{\rm SG}^{\rm (W)} &= \frac{1}{12}(\mu_{\rm B}^4/J_0^2), \end{aligned}\right\} \quad \text{for} \quad z = 6. \tag{4.20}$$

By comparing the results of the mean-field approximation (4.19)-(4.20) with that of the Bethe approximation (4.13)-(4.14), it can be concluded that the transition points of the latter are lower than those of the former and the coefficients $\{\overline{\chi}_{\rm SG}\}$ are greater accordingly. This observation can be expected from the CAM[6-8]: See Section 5.

4.2 The Second Approximation (the "Square Approximation")

Next, as the second approximation[10], consider the four spins around a plaquette and the nearest-neighbouring sites of them: See Figure 9. The Hamiltonian of this cluster is as follows:

$$\begin{aligned} \mathcal{H}_\Omega \equiv \; & - \; (J_{0,1}\sigma_0\sigma_1 + J_{1,2}\sigma_1\sigma_2 + J_{2,3}\sigma_2\sigma_3 + J_{3,0}\sigma_3\sigma_0) \\ & - \; \sum_{i=0}^{3}\sum_{k=1}^{z-2} J_{i,ik}\sigma_i\sigma_{ik}. \end{aligned} \tag{4.21}$$

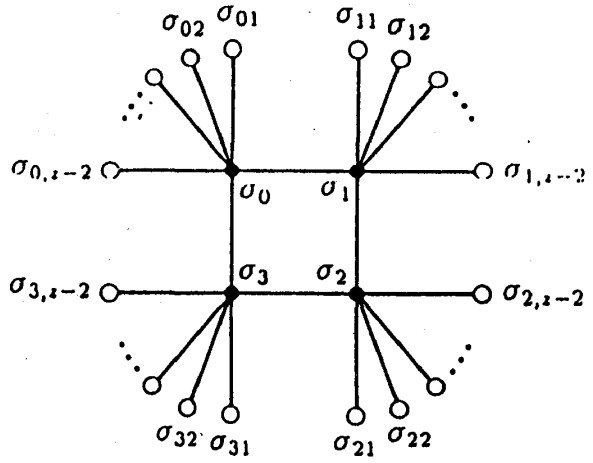

Figure 9: The cluster used in the "square approximation".

The effective-fields are applied on the boundary sites

$$\partial\Omega \equiv \{\sigma_{ik} | i = 0, 1, 2, 3,\ k = 1, 2, \cdots, z-2\}. \tag{4.22}$$

As the following calculations involve a "frustration" explicitly, in some sense, properties of spin glasses emerge after this approximation for the first time.

Some correlation functions with respect to this Hamiltonian are obtained as follows or diagrammatically shown in Figure 10:

$$\begin{aligned} \langle\sigma_0\sigma_1\rangle_{\Omega 0} &= \frac{A_{0,1}t + A_{0,3}A_{3,2}A_{2,1}t^3}{1 + A_{0,1}A_{1,2}A_{2,3}A_{3,0}t^4} \\ &= A_{0,1} \cdot \frac{t + \Phi t^3}{1 + \Phi t^4}, \end{aligned} \tag{4.23}$$

$$\begin{aligned} \langle\sigma_0\sigma_2\rangle_{\Omega 0} &= \frac{A_{0,1}A_{1,2}t^2 + A_{0,3}A_{3,2}t^2}{1 + A_{0,1}A_{1,2}A_{2,3}A_{3,0}t^4} \\ &= A_{0,1}A_{1,2} \cdot \frac{t^2 + \Phi t^2}{1 + \Phi t^4}, \end{aligned} \tag{4.24}$$

where Φ denotes whether a frustration exists on the plaquette at the centre of

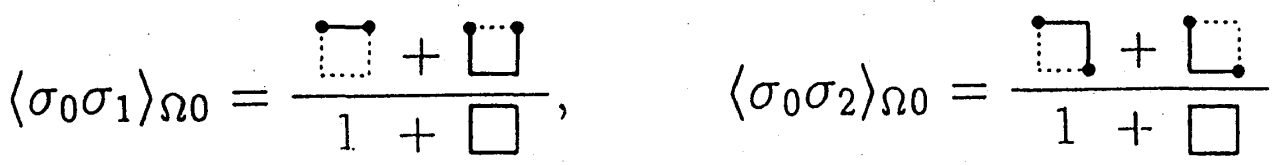

Figure 10: Diagrams for some correlation functions.

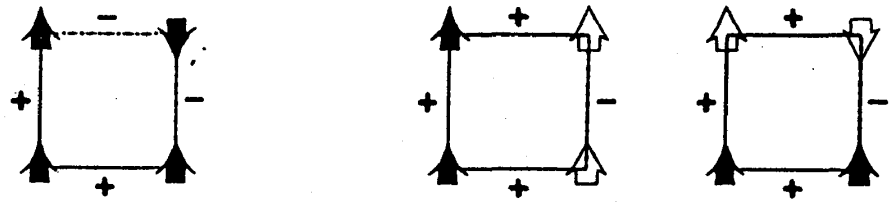

Figure 11: A non-frustrated plaquette and a frustrated one.

the cluster:

$$\Phi \equiv A_{0,1}A_{1,2}A_{2,3}A_{3,0}. \tag{4.25}$$

When $\Phi = +1$, the four spins on the plaquette do not frustrate, and when $\Phi = -1$, they do: See Figure 11. We obtain from (4.23) and (4.24)

$$\langle \sigma_0\sigma_1 \rangle^2_{\Omega 0} = \left(\frac{t + \Phi t^3}{1 + \Phi t^4} \right)^2, \tag{4.26}$$

$$\langle \sigma_0\sigma_2 \rangle^2_{\Omega 0} = \left(\frac{t^2 + \Phi t^2}{1 + \Phi t^4} \right)^2. \tag{4.27}$$

These expressions mean that the squares of the correlation functions do not depend on configurations of interactions perfectly, but depends only on Φ, or on configurations of the frustration. This statement holds for more general system: See Appendix A.

To take the quenched-averages of (4.26) and (4.27), we must know only the probability of $\Phi = +1$ and that of $\Phi = +1$. They are easily obtained as

$$P(\Phi = +1) = \frac{1}{2}, \tag{4.28}$$

$$P(\Phi = -1) = \frac{1}{2}. \tag{4.29}$$

Also in larger systems with the probability distribution of interactions in the form (4.1), the probabilities that a frustration exists or does not exist on a plaquette are, in general, $\frac{1}{2}$ independently of configurations of frustrations on the other plaquettes except a restriction in the 3- and higher dimensional systems. Now we obtain[10]

$$G_{01}(t) \equiv [\langle \sigma_0\sigma_1 \rangle^2_{\Omega 0}]_{\text{av.}} = \frac{1}{2} \left\{ \left(\frac{t + t^3}{1 + t^4} \right)^2 + \left(\frac{t - t^3}{1 - t^4} \right)^2 \right\}, \tag{4.30}$$

$$G_{02}(t) \equiv [\langle \sigma_0\sigma_2 \rangle^2_{\Omega 0}]_{\text{av.}} = \frac{1}{2} \left(\frac{2t^2}{1 + t^4} \right)^2. \tag{4.31}$$

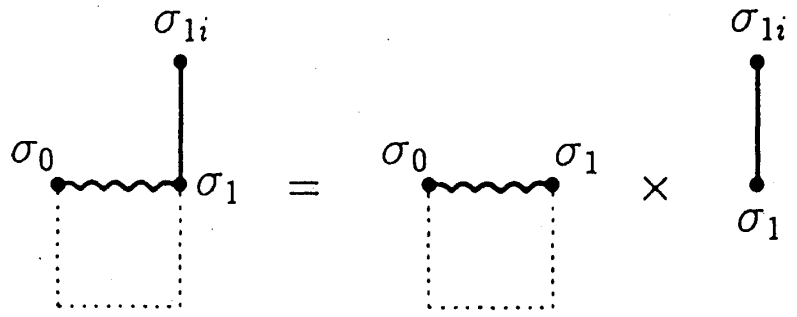

Figure 12: Decomposition of a correlation function.

Another correlation function is given[10] by

$$\begin{aligned}[\langle\sigma_0\sigma_{1i}\rangle^2_{\Omega 0}]_{\rm av.} &= [\langle\sigma_0\sigma_1\rangle^2_{\Omega 0}]_{\rm av.}[\langle\sigma_1\sigma_{1i}\rangle^2_{\Omega 0}]_{\rm av.} \\ &= G_{01}\cdot t^2, \end{aligned} \tag{4.32}$$

or diagrammatically shown in Figure 12. In general, for a system which consists of two clusters contacting with each other at only one site, the quenched-averages of the squares of correlation functions between one site on one cluster and one on another cluster can be decomposed[10] in the paramagnetic phase as (4.32): See Appendix B.

Now we can calculate (2.39)-(2.42) explicitly as follows:

$$\begin{aligned} B_0 &\equiv \sum_{J\in\Omega}[\langle\sigma_0\sigma_J\rangle^2_{\Omega 0}]_{\rm av.} \\ &= \{1+(z-2)t^2\}\{1+2G_{01}+G_{02}\}, \end{aligned} \tag{4.33}$$

$$\begin{aligned} B_1 &\equiv \sum_{J\in\Omega}[\langle\sigma_i\sigma_J\rangle^2_{\Omega 0}]_{\rm av.} \\ &= 1-t^4+\{1+(z-2)t^2\}\{1+2G_{01}+G_{02}\}t^2, \end{aligned} \tag{4.34}$$

$$\begin{aligned} C_0 &\equiv \sum_{j\in\partial\Omega}[\langle\sigma_0\sigma_i\rangle^2_{\Omega 0}]_{\rm av.} \\ &= (z-2)\{1+2G_{01}+G_{02}\}t^2, \end{aligned} \tag{4.35}$$

and

$$\begin{aligned} C_1 &\equiv \sum_{j\in\partial\Omega}[\langle\sigma_i\sigma_j\rangle^2_{\Omega 0}]_{\rm av.} \\ &= 1-t^4+(z-2)\{1+2G_{01}+G_{02}\}t^4, \end{aligned} \tag{4.36}$$

respectively. The transition point is determined by the equation

$$C_0 = C_1 \quad \text{at } T = T_{\rm SG}. \tag{4.37}$$

Also the spin-glass susceptibility is given by Equation (2.37). The numerical results of them are as follows[10]: In the 2-dimensional system, we have

$$\left.\begin{aligned} T_{\rm SG}^{\rm (SQ)} &= 1.45543(J_0/k_{\rm B}), \\ \overline{\chi}_{\rm SG}^{\rm (SQ)} &= 0.48918(\mu_{\rm B}^4/J_0^2), \end{aligned}\right\} \quad \text{for} \quad z=4, \tag{4.38}$$

and in the 3-dimensional system, we obtain

$$\left.\begin{array}{l} T_{\rm SG}^{\rm (SQ)} = 2.06404(J_0/k_{\rm B}), \\ \overline{\chi}_{\rm SG}^{\rm (SQ)} = 0.16880(\mu_{\rm B}^4/J_0^2), \end{array}\right\} \quad \text{for} \quad z = 6. \tag{4.39}$$

Comparing these values with (4.19)-(4.20) and (4.13)-(4.14), it can again be observed that improvements of the approximation cause successive decrease in $T_{\rm SG}$ and increase in $\overline{\chi}_{\rm SG}$.

4.3 Numerical Results of the 2- and 3-Dimensional Systems

Further calculations were done by the brick-laying transfer method[8] on computers.

The treated clusters of the 2-dimensional system are listed in Figure 13. All the results obtained from them are listed in Table 1. Also the treated clusters of the 3-dimensional system are listed in Figure 14, the results in Table 2.

Table 1: Results of the 2-dimensional system.

cluster†	$T_{\rm SG}(J_0/k_{\rm B})$	$\overline{\chi}_{\rm SG}(\mu_{\rm B}^4/J_0^2)$	$\log T_{\rm SG}$	$\log \overline{\chi}_{\rm SG}$
$2D-a$	2.00000	0.12500	0.693147	-2.07944
b	1.51865	0.38017	0.417822	-0.96714
c	1.45543	0.48918	0.375301	-0.71503
d	1.34379	0.77969	0.295494	-0.24886
e	1.23795	1.31524	0.213457	-0.27402
f	1.17823	1.77188	0.164013	-0.57204
g	1.04629	3.76646	0.045251	1.32614

†) The symbols $a, b, \cdots$ denote the clusters in Figure 13.

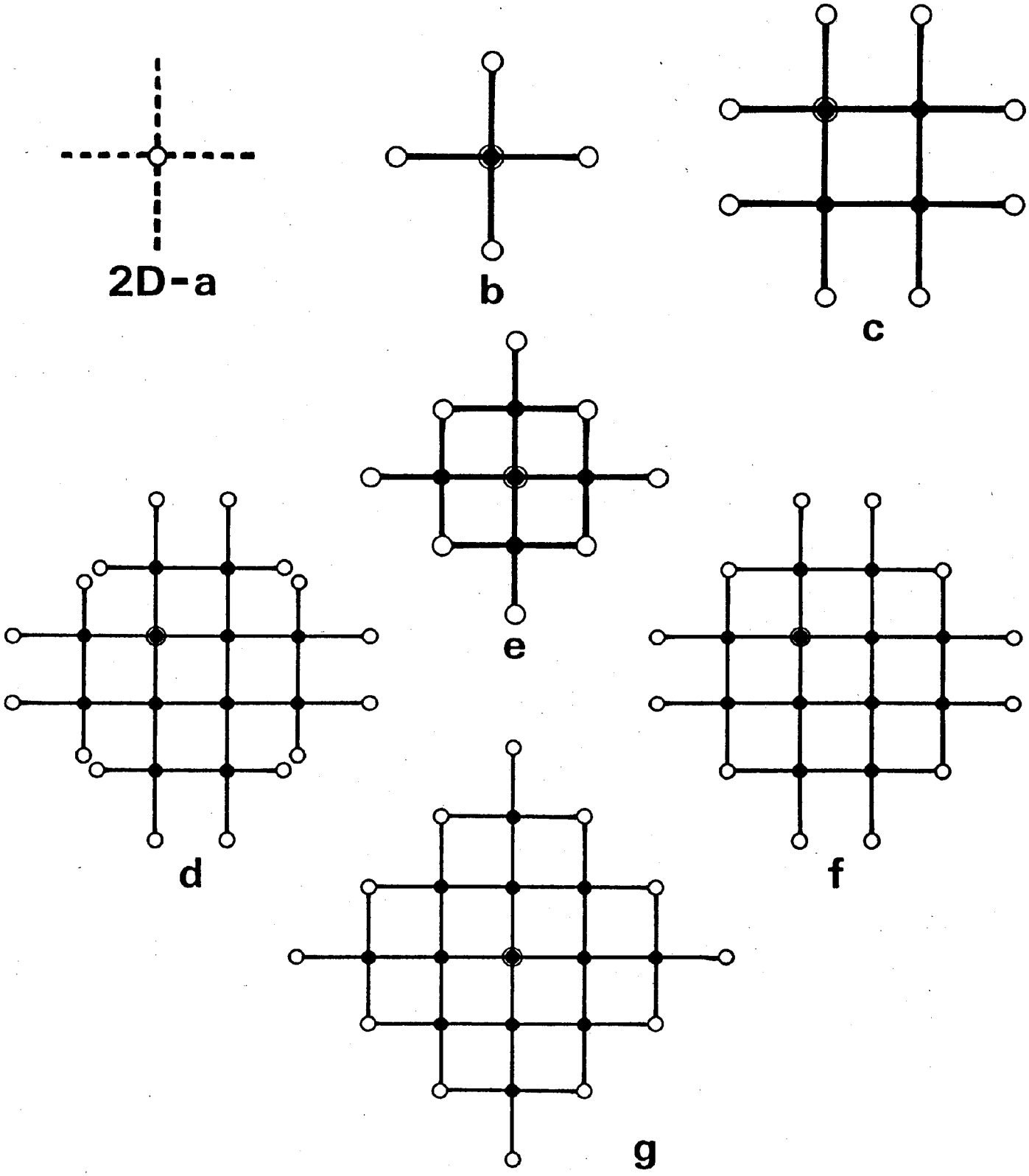

Figure 13: Treated clusters of the 2-dimensional system. The symbol "o" denotes the boundary sites of the clusters.

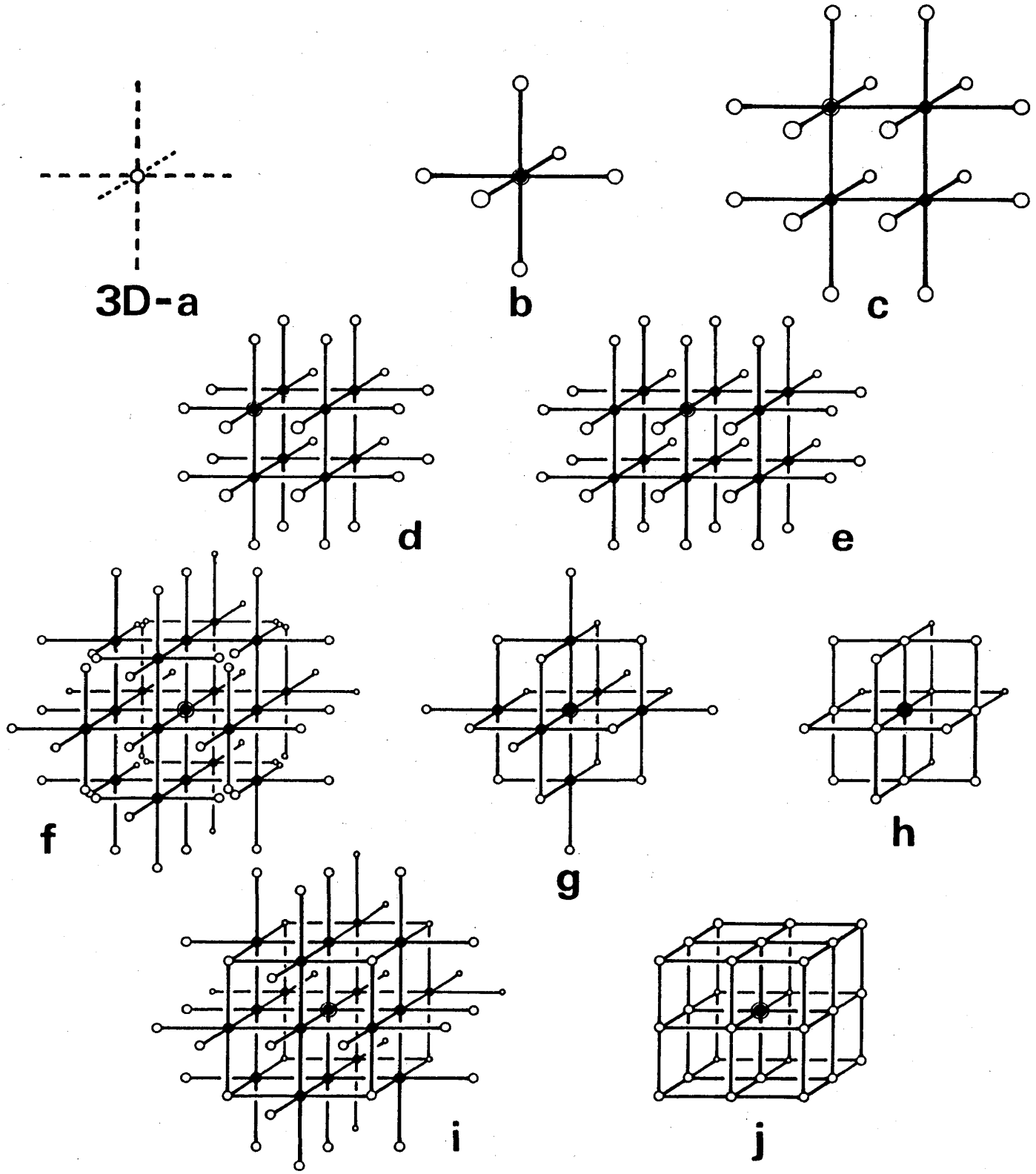

Figure 14: Treated clusters of the 3-dimensional system. The symbol "o" denotes the boundary sites of the clusters.

Table 2: Results of the 3-dimensional system.

$cluster^{\dagger}$	$T_{SG}(J_0/k_B)$	$\overline{\chi}_{SG}(\mu_B^4/J_0^2)$	$\log(T_{SG}-1.2)$	$\log\overline{\chi}_{SG}$
$3D-a^{[10]}$	2.44949	0.08333	0.22274	-2.48491
$b^{[10]}$	2.07809	0.16140	-0.13000	-1.82385
$c^{[10]}$	2.06404	0.16880	-0.14614	-1.77907
d	2.03051	0.18825	-0.18572	-1.66999
e	2.00434	0.20459	-0.21773	-1.58719
f	1.97693	0.21892	-0.25241	-1.51904
g	1.92534	0.27110	-0.32112	-1.30528
h	1.79015	0.50646	-0.52738	-0.68030
$i^{\ddagger}$	1.892(4)	0.304(3)	-0.368(6)	-1.189(4)
$j^{\ddagger}$	1.710(5)	0.725(18)	-0.674(10)	-0.321(26)

†) The symbols $a, b, \cdots$ denote the clusters in Figure 14.

‡) For these clusters, we take the quenched-averages of samples which are randomly chosen out of all, because of the limit of the computational time and memories; about 0.03% out of all for the cluster i, and about 0.17% for the cluster j are chosen.

5 Analyses by the Coherent-Anomaly Method (CAM)

In the present section, data listed in Section 4 are analysed using the Coherent-Anomaly Method[6-8] proposed by Suzuki. The spin-glass transition points and the critical exponents γ_s of the 2- and 3- dimensional systems are mentioned.

5.1 The Theory of the Coherent-Anomaly Method

First, the CAM is briefly reviewed.

Consider a critical phenomenon. Near and above the transition point $T_c^{(*)}$, the response function of the order parameter to an applied field is expected to show such behaviour as

$$\chi^{(*)}(T) \simeq \frac{C}{(T-T_c^{(*)})^{\gamma}} \quad \text{as} \quad T \to T_c^{(*)}+0, \tag{5.1}$$

with the fractional exponent

$$\gamma > 1. \tag{5.2}$$

On the other hand, ordinary effective-field theories, which pay attention only to the linear response, yield the "classical", or "Landau-type" behaviour of the response function as shown in Section 2:

$$\chi^{(n)} \simeq \overline{\chi}^{(n)} \cdot \frac{T_c^{(n)}}{T - T_c^{(n)}} \quad \text{as} \quad T \to T_c^{(n)} + 0, \tag{5.3}$$

with

$$T_c^{(n)} > T_c^{(*)}, \tag{5.4}$$

$$\gamma = 1, \tag{5.5}$$

where n specifies a type of the approximation.

Consider a series of approximations; $n = 1, 2, 3, \ldots$ If the series converges to the true system, or

$$\lim_{n\to\infty} T_c^{(n)} = T_c^{(*)}, \tag{5.6}$$

$$\lim_{n\to\infty} \chi^{(n)}(T) = \chi^{(*)}(T) \qquad \text{for} \quad {}^{\forall}T > T_c^{(*)}, \tag{5.7}$$

the discrepancy between the exponents (5.2) and (5.5) is expected to cause the anomaly of $\overline{\chi}$:

$$\overline{\chi}^{(n)} \to \infty \quad \text{as} \quad n \to \infty, \text{ or } T_c^{(n)} \to T_c^{(*)} + 0. \tag{5.8}$$

For not only the spin-glass but general phase-transitions, Suzuki proposed that there may exist some systematic series of approximations for which the residue $\overline{\chi}$ can be written in the form[6-7]

$$\overline{\chi}^{(n)} \simeq \frac{C'}{(T_c^{(n)} - T_c^{(*)})^{\psi}} \quad \text{as} \quad n \to \infty, \text{ or } T_c^{(n)} \to T_c^{(*)} + 0, \tag{5.9}$$

and correspondingly, the response function takes the form

$$\chi^{(n)} \simeq \frac{C'}{(T_c^{(n)} - T_c^{(*)})^{\psi}} \cdot \frac{T_c^{(n)}}{T - T_c^{(n)}} \quad \text{as} \quad \begin{cases} T_c^{(n)} & \to & T_c^{(*)} + 0, \\ T & \to & T_c^{(*)} + 0. \end{cases} \tag{5.10}$$

This behaviour is called the "coherent-anomaly", and the series which shows this anomaly is called a "canonical series". After some discussions[6-7] using the "envelope theory" or the "finite-degree-of-approximations scaling", which is analogous to Fisher's finite-size scaling theory[22], the "coherent-anomaly relation" can be derived as follows[6-7]:

$$\gamma = \psi + 1. \tag{5.11}$$

According to the above discussions, fitting some numerical data

$$\begin{array}{llll} T_c^{(1)}, & T_c^{(2)}, & T_c^{(3)}, & \ldots, \\ \overline{\chi}^{(1)}, & \overline{\chi}^{(2)}, & \overline{\chi}^{(3)}, & \ldots, \end{array} \tag{5.12}$$

to the function (5.9) may give the true critical-exponent γ with rather good accuracy using the relation (5.11). The CAM has been applied to such critical phenomena as the ferromagnetic and the chiral transition[12], and yields the good results: See the references of Ref.[11].

5.2 Data Analyses

In the following, the results of applications of the CAM to the data listed in Section 4 are mentioned.

Consider a temperature-dependent variable $x(T)$. If this variable can be expanded as

$$x - x_{\rm SG} \equiv x(T) - x(T_{\rm SG}) \simeq \alpha(T - T_{\rm SG}) \tag{5.13}$$

near $T \simeq T_{\rm SG}$, then the spin-glass susceptibility near and above the transition point, $T \to T_{\rm SG}^{(*)} + 0$, can be written using the variable x in the form

$$\begin{aligned} \chi_{\rm SG}^{(*)}(T) &\simeq \frac{C}{(T - T_{\rm SG}^{(*)})^{\gamma_s}} \\ &\simeq \frac{C\alpha_s^{\gamma}}{\left|x - x_{\rm SG}^{(*)}\right|^{\gamma_s}}. \end{aligned} \tag{5.14}$$

The same discussion as in Section 5.1 can be applied[6] to the variable x too. The spin-glass susceptibility derived in Section 2 and Section 3 can be represented in the form

$$\chi_{\rm SG} = \beta^2 \frac{G(x)}{F(x)}. \tag{5.15}$$

Then near and above the spin-glass transition point $x_{\rm SG}$, which is determined by

$$F(x_{\rm SG}) = 0, \tag{5.16}$$

the spin-glass susceptibility behaves as

$$\begin{aligned} \chi_{\rm SG}(x) &\simeq \frac{1}{T_{\rm SG}^2} \cdot \frac{G(x_{\rm SG})}{(x - x_{\rm SG})\frac{d}{dx}F(x_{\rm SG})} \\ &= \frac{1}{T_{\rm SG}^2} \left| \frac{G(x_{\rm SG})}{x_{\rm SG}\frac{d}{dx}F(x_{\rm SG})} \right| \cdot \frac{1}{\epsilon} \quad \text{as} \quad \epsilon \to 0, \end{aligned} \tag{5.17}$$

where

$$\epsilon \equiv \left| \frac{x - x_{\rm SG}}{x_{\rm SG}} \right|. \tag{5.18}$$

The coefficient $\overline{\chi}_{\rm SG}$ can be defined as follows[6]:

$$\overline{\chi}_{\rm SG}(x_{\rm SG}) \equiv \frac{1}{T_{\rm SG}^2} \left| \frac{G(x_{\rm SG})}{x_{\rm SG}\frac{d}{dx}F(x_{\rm SG})} \right|. \tag{5.19}$$

Of course, this can be transformed from $\overline{\chi}_{\rm SG}(T_{\rm SG})$ easily by the formula

$$\overline{\chi}_{\rm SG}(x_{\rm SG}) = |\alpha| \frac{T_{\rm SG}}{x_{\rm SG}} \cdot \overline{\chi}_{\rm SG}(T_{\rm SG}). \tag{5.20}$$

According to the CAM theory, $\overline{\chi}_{\rm SG}$ may show[6] the coherent anomaly:

$$\overline{\chi}^{(n)}_{\rm SG}(x^{(n)}_{\rm SG}) \simeq \frac{C''}{\left|x^{(n)}_{\rm SG} - x^{(*)}_{\rm SG}\right|^{\psi}} \quad \text{as} \quad n \to \infty, \text{ or } \left|x^{(n)}_{\rm SG} - x^{(*)}_{\rm SG}\right| \to 0. \tag{5.21}$$

When a series of approximations is canonical enough to show the coherent-anomaly, data of $T^{(*)}_{\rm SG}$ and ψ derived from the CAM-analyses are expected not to depend on the choice of the variable x. In the following analyses of the 3-dimensional system, the variables

$$x = T, \ \tanh\left(\frac{1}{T}\right), \ e^{-\frac{1}{T}} \tag{5.22}$$

are used.

5.2.1 The 2-Dimensional System

In the 2-dimensional spin-glass system of Ising spins, the conclusion that $T^{(*)}_{\rm SG} \equiv 0$ is now quite acceptable. By the way, there are two types of the definition of the response function; the Edwards-Anderson susceptibility as

$$\chi_{\rm EA} \equiv \frac{1}{N} \cdot \sum_{i,j} [\langle \sigma_i \sigma_j \rangle^2]_{\rm av.}, \tag{5.23}$$

and the spin-glass susceptibility as

$$\chi_{\rm SG} \equiv \frac{\beta^2}{N} \cdot \sum_{i,j} [\langle \sigma_i \sigma_j \rangle^2]_{\rm av.}. \tag{5.24}$$

In the case of $T^{(*)}_{\rm SG} \equiv 0$, there exists discrepancy between the critical exponents of the singularity of (5.23) and (5.24) as follows:

$$\chi_{\rm EA} \propto \frac{1}{T^{\gamma_s}}, \tag{5.25}$$

$$\chi_{\rm SG} \propto \frac{1}{T^{\tilde{\gamma}_s}}, \tag{5.26}$$

with

$$\tilde{\gamma}_s = \gamma_s + 2. \tag{5.27}$$

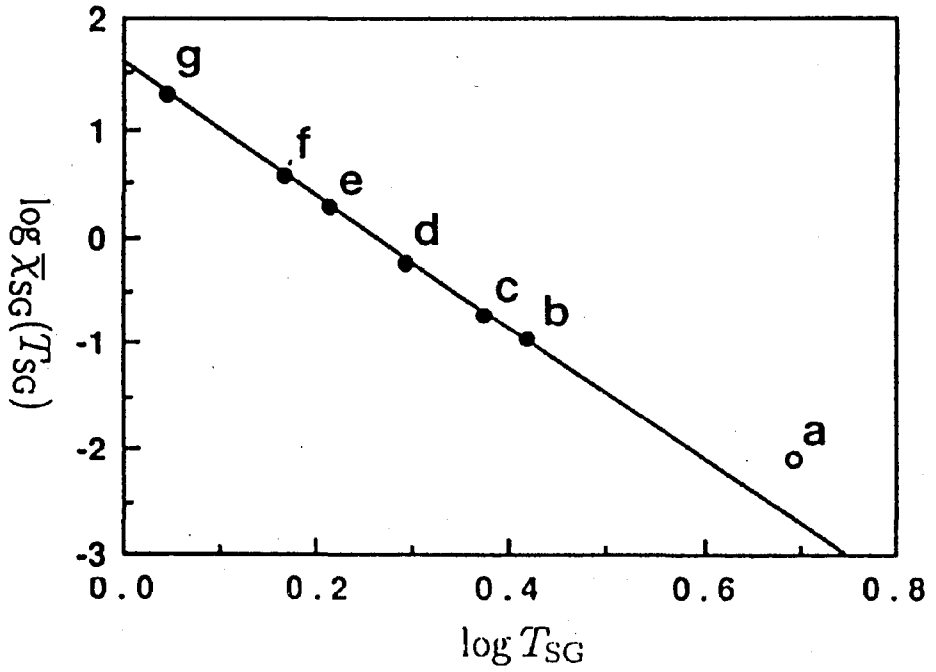

Figure 15: The data points *b*-*g* are fitted to the function

$$\log \overline{\chi}_{SG} = -5.16 \log(T_{SG}) + 1.6.$$

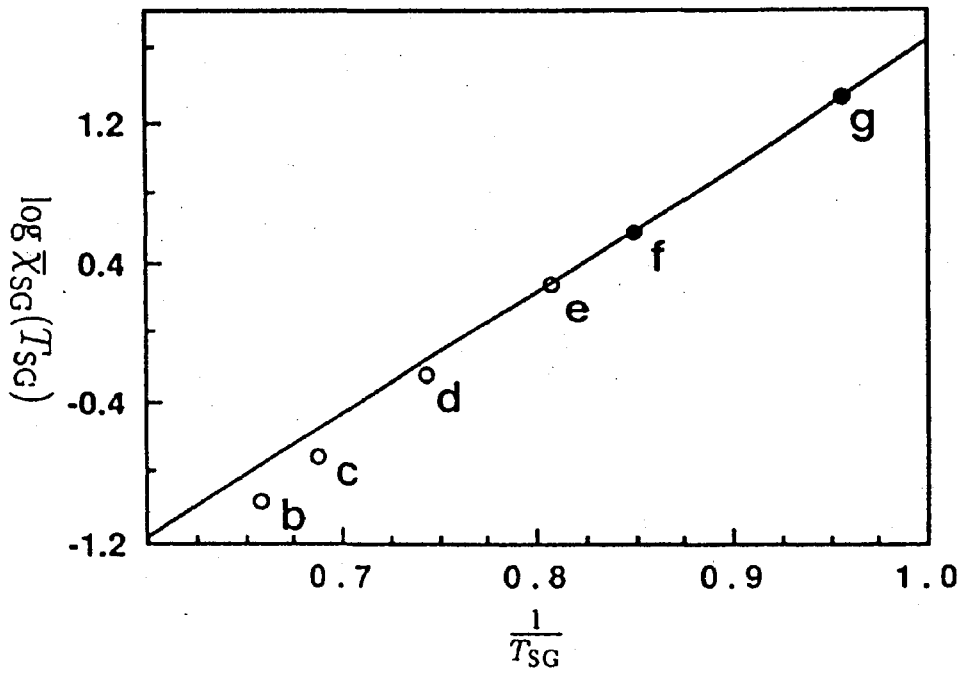

Figure 16: The data points *b*-*g* are fitted to the function

$$\log \overline{\chi}_{SG} = 7.1/T_{SG} - 5.4.$$

Table 3: The CAM-analyses of the 2-dimensional system.

data points†	$\log \overline{\chi} = -\psi \log(T_{\rm SG} - T_{\rm SG}^{(*)}) + C$		*fitting with* $T_{\rm SG}^{(*)} \equiv 0$
	$\gamma_{\rm s} = \psi + 1$‡	$T_{\rm SG}^{(*)}(J_0/k_{\rm B})$‡	$\gamma_{\rm s} = \tilde{\psi} - 1$‡⋆
a to g	3.7(3)	0.68(7)	4.3(3)
b to g	6.0(3)	0.22(7)	5.16(5)
b, c, e, f, g	6.2(2)	0.20(4)	5.14(4)
d, e, f, g	7(1)	0.03(22)	5.28(4)
b, e, g	6.32	0.171	5.15(5)
c, d, f	4.71	0.510	5.11(1)
e, f, g	4.84	0.439	5.27(7)

†) The data-points $a, b, \cdots$ denote the clusters in Figure 13.
‡) Errors of these data are estimated from the errors appearing in the least-square-fitting to the functions.
⋆) $\tilde{\psi} = \tilde{\gamma}_{\rm s} - 1 = \gamma_{\rm s} + 1$: See the relation (5.27).

In the present thesis, we use the definition $\chi_{\rm SG}$, but generally the definition $\chi_{\rm EA}$ is used.

The results of the least-square-fitting of the data on the 2-dimensional system (Table 1) to the function (5.21) are shown in Table 3. Also some examples of the fitting are plotted in Figures 15 and 16. The variables $\tanh(1/T)$, and $\exp(-1/T)$ cannot be used to analyse them, because of the impossibility of the expansion (5.13).

5.2.2 The 3-Dimensional System

The results obtained from the data on the 3-dimensional system (Table 2) are also shown in Table 4. In the least-square-fitting of data on the 3-dimensional system, a difficulty arises: Data only on the clusters h and j have statistical errors because of the Monte-Carlo-sampling. The present analyses are made using the statistical errors for data on the clusters h and j, and using the errors appearing in the least-square-fitting for data on other clusters. This method is, however, still open to discussions, because they are of different types of errors. Some plots are shown in Figures 17, 18, and 19.

Table 4: The CAM-analyses of the 3-dimensional system. The fitting function used here is

$$\log \overline{\chi}_{\rm SG}^{(n)}(x_{\rm SG}^{(n)}) = -\psi \log \left| x_{\rm SG}^{(n)} - x_{\rm SG}^{(*)} \right| + C.$$

data point†	*used variable* x					
	$x \equiv T$		$x \equiv \tanh\left(\frac{1}{T}\right)$		$x \equiv e^{-\frac{1}{T}}$	
	$\gamma_s^{\ddagger}$	$T_{\rm SG}^{(*)}\left(\frac{J_0}{k_B}\right)^{\ddagger}$	$\gamma_s^{\ddagger}$	$T_{\rm SG}^{(*)\ddagger}$	$\gamma_s^{\ddagger}$	$T_{\rm SG}^{(*)\ddagger}$
a to j	2.46(6)	1.51(2)	3.0(1)	1.45(2)	3.9(1)	1.39(2)
b to j	3.2(2)	1.36(5)	4.5(6)	1.22(9)	5.8(8)	1.15(9)
b, c, d, f to j	3.2(2)	1.35(5)	——	——	——	——
b, c, d, g, i	4.70(1)	0.913(3)	——	——	——	——
b, c, d, h, j	3.30(3)	1.343(8)	5.2(1)	1.14(2)	6.8(2)	1.06(2)
f, g, h, i, j	6.9(3.9)	0.5(8)	——	——	——	——

†) The data-points $a, b, \cdots$ denote the clusters in Figure 14.
‡) Errors of these data are estimated from the errors appearing in the least-square-fitting to the functions.

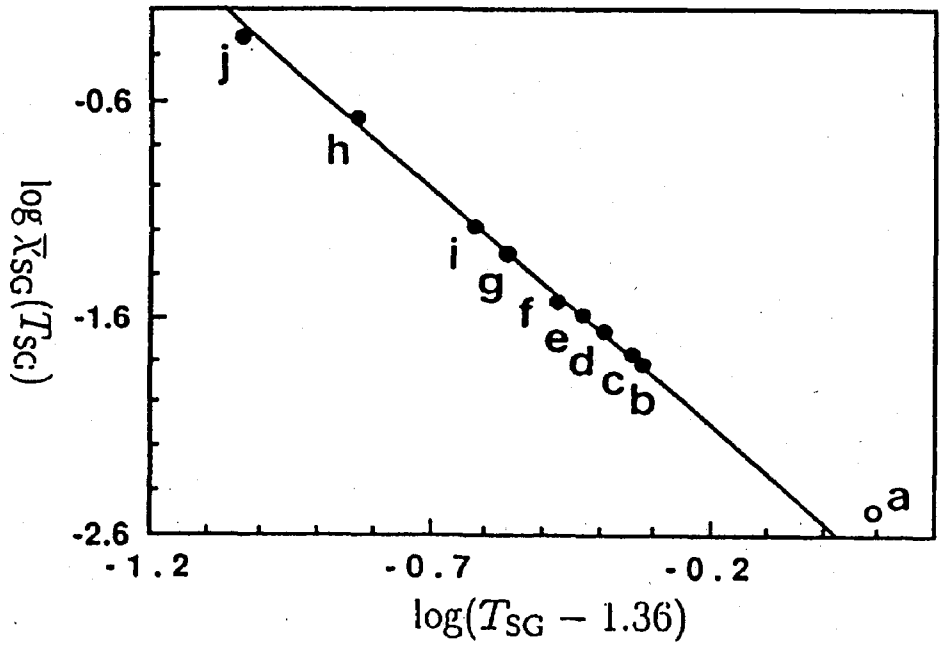

Figure 17: The data point b-g are fitted to the function

$$\log \overline{\chi}_{\rm SG} = -2.2 \log(T_{\rm SG} - 1.36) - 2.5.$$

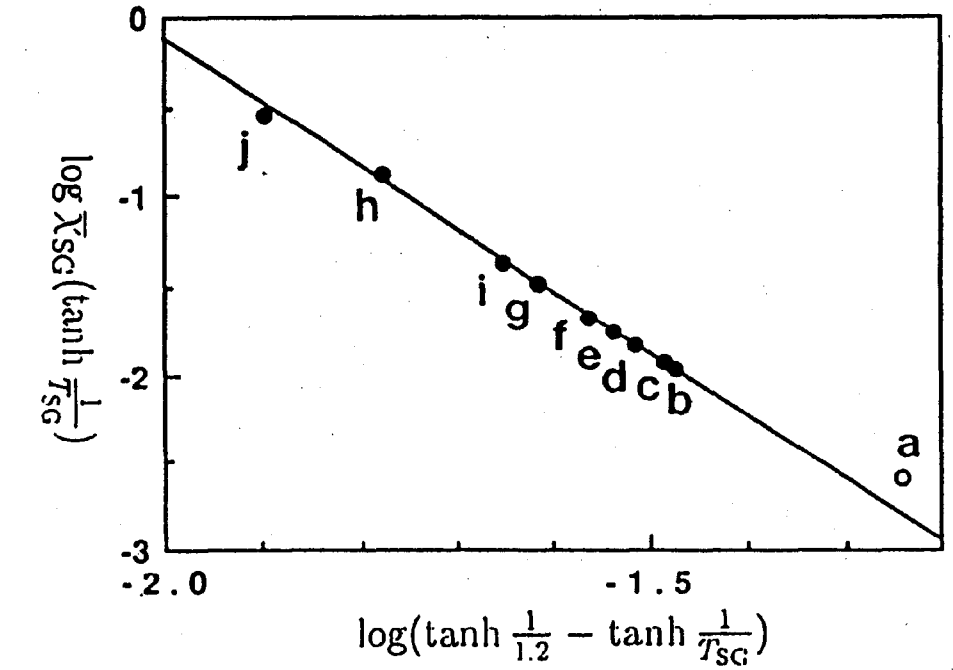

Figure 18: The data point b-g are fitted to the function

$$\log \overline{\chi}_{SG} = -3.5 \log\{\tanh(1/1.22) - \tanh(1/T_{SG})\} - 7.2.$$

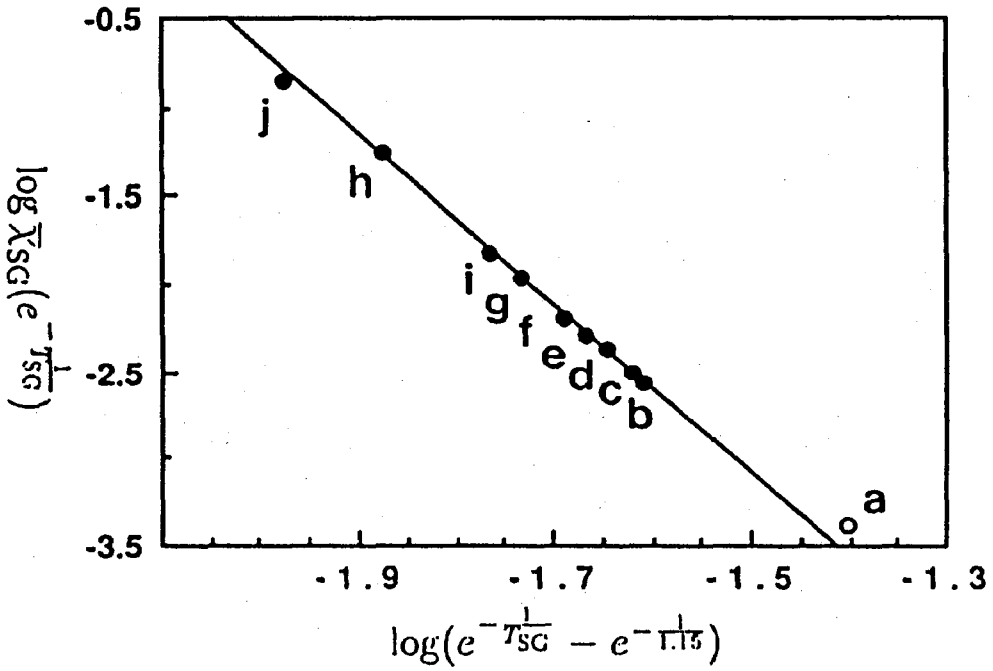

Figure 19: The data point b-g are fitted to the function

$$\log \overline{\chi}_{SG} = -4.8 \log\{\exp(-1/T_{SG}) - \exp(-1/1.15)\} - 10.3.$$

6 Discussions and Summary

6.1 Conclusion for the 2-Dimensional System

In the 2-dimensional system, it can be concluded that the assumption of $T_{\rm SG}^{(*)} \equiv 0$ yields a better conclusion.

1. Figure 15 suggests that we had better excluded the point a of the "Weiss approximation". The Weiss approximation may not take part in the "canonical series" of the effective-field theory.

2. Taking the point d into account reduces the degree of the fitness.

3. We can fit the points b, e, and g well. Each of the series b-e-g and c-f may be a part of different canonical-series.

4. When we set both ψ and $T_{\rm SG}^{(*)}$ being free parameters and fit the data to the function
$$\log \overline{\chi}_{\rm SG} = -\psi \log(T_{\rm SG} - T_{\rm SG}^{(*)}) + c, \tag{6.1}$$
we may obtain
$$T_{\rm SG}^{(*)} \simeq 0.2\ (J_0/k_{\rm B}), \tag{6.2}$$
and
$$\gamma_{\rm s} \simeq 6. \tag{6.3}$$

5. When we set $T_{\rm SG}^{(*)} \equiv 0$ as in most studies and fit the data to the function (6.1), we obtain
$$\gamma_{\rm s} \simeq 5, \tag{6.4}$$
and especially, using the points b-e-g we obtain
$$\gamma_{\rm s} = 5.15(5) \quad \text{for} \quad T_{\rm SG}^{(*)} \equiv 0 : \tag{6.5}$$
See Figure 15. These are in good agreement with the data[30] of the high-temperature-expansion: See Table 5.

6. The data are also fitted to the function
$$\log \overline{\chi}_{\rm SG} = \frac{c_1}{T_{\rm SG}} - c_2 : \tag{6.6}$$
See Figure 16. The linearity of this fitting is worse than that of the fitting to the function (6.1). The last two data-points f, and g yield the values
$$\begin{cases} c_1 &= 7.05, \\ c_2 &= 5.41. \end{cases} \tag{6.7}$$

Table 5: Recent studies of the 2-dimensional $\pm J$ model.

authors	*method*†	*conclusion*		
Morgenstern-Binder('79-'80)[23]	MC sim.	$T_{SG}^{(*)} \equiv 0$		
Morgenstern('82)[24]	TM + MC calc.	$T_{SG}^{(*)} \equiv 0$		
		exponents⋆ *assuming* $T_{SG}^{(*)} \equiv 0$		
		γ_s	ν	η
Binder('82)[25]	MC sim.	~ 4	~ 2	——
Young('83)[26]	MC sim.	~ 4	~ 2	——
McMillan('83)[27]	MC sim.	4.5(5)‡	2.64(23)	0.28(4)
Cheung-McMillan('83)[28]	TM + FSS	——	2.59(13)	——
Young('84)[29]	MC sim. $68^2, 128^2$	4.1	2.75	——
Singh-Chakraverty('86)[30]	HTE up to w^{19}	5.3(3)	——	——
Bhatt-Young('88)[31]	sim. + FSS	4.6(5)‡	2.6(4)	0.20(5)

†) "MC" denotes Monte Carlo. "TM" denotes the transfer-matrix method. "FSS" denotes the finite-size-scaling. "HTE" denotes the high-temperature expansion in $w \equiv \tanh^2(1/T)$.

‡) These γ_s are obtained from the scaling relation $\gamma_s = (2-\eta)\nu$.

⋆) To know the definition of the exponents, see Appendix C.

Recent studies[23-31] concerning the critical exponents of the 2-dimensional $\pm J$ model with Ising spins are listed in Table 5. For this system, the result $T_{SG}^{(*)} \equiv 0$ had been almost confirmed till 1982, and after that, studies on this assumption have been developed. As the error bars of data in the last two rows[30-31] of Table 5 overlap with each other, it is plausible that $\gamma_s \simeq 5$. The present result confirms this conclusion.

6.2 Conclusion for the 3-Dimensional System

Results of the 3-dimensional system have ambiguity. It is difficult to conclude them with a firm value.

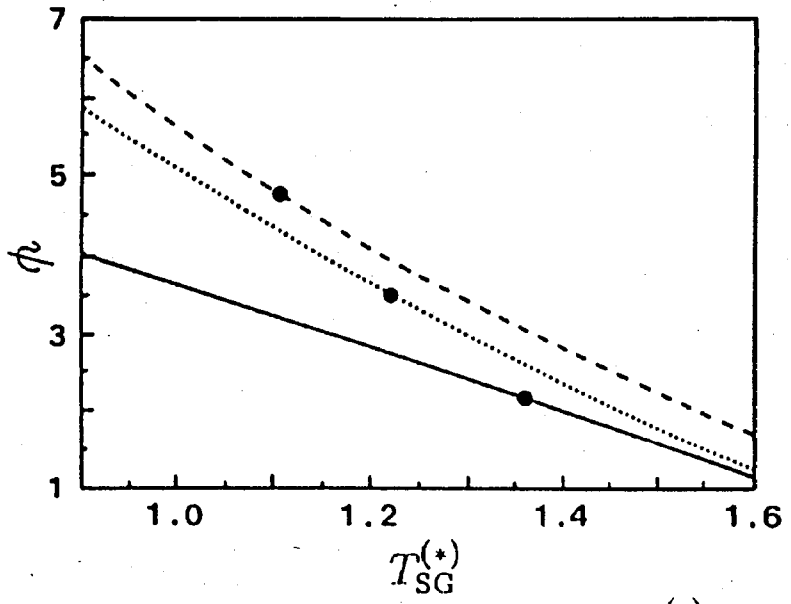

Figure 20: The values ψ fitted under the fixed values $T_{SG}^{(*)}$. Fitting variables are T_{SG} (*the solid line*), $\tanh\frac{1}{T_{SG}}$ (*the dotted line*), and $e^{-\frac{1}{T_{SG}}}$ (*the broken line*). The symbols "•" indicate the values of the best fittings.

1. As in the 2-dimension system, the data of the "Weiss approximation" do not seem to fit to the other data: See Figure 17 .

2. On the other hand, also the data point j does not seem to fit to the other data. It is a possible case that the series of approximations has not converged enough to show the coherent-anomaly.

3. As for fitting the data using the variable $x = T$, it seems to be plausible to conclude that
$$T_{SG}^{(*)} \sim 1.3\ (J_0/k_B), \tag{6.8}$$
and
$$\gamma_s > 3, \tag{6.9}$$
but the data using the variables $\tanh(1/T)$ and $e^{-1/T}$ suggest some other values: See Table 4 and Figures 17, 18 and 19. The values ψ fitted for some fitting variables under the fixed values $T_{SG}^{(*)}$ are plotted in Figure 20. The curves do not agree with each other. This indicates that the series of the approximations is not canonical enough. Besides, these data do not agree with the recent results by other authors: See below.

4. The fractional behaviour which characterizes the 3-dimensional system may emerge after more body-like clusters such as the cluster j for the first time. In other words, calculations of larger clusters may be needed to observe

Table 6: Recent studies of the 3-dimensional $\pm J$ model.

authors	*method*†	$T_{\rm SG}\left(\frac{J_0}{k_{\rm B}}\right)$	*exponents*⋆		
			$\gamma_{\rm s}$	ν	η
Young('84)[29]	MC sim. 64^3	≤ 1.0	2.9◇	1.2◇	−0.4◇
Ogielski-Morgenstern('85)[32]	MC sim. 64^3	1.20(5)	~ 2.4‡	1.2(1)	−0.1(1)
Bhatt-Young('85)[33]	MC sim. $3^3 \sim 20^3$	$1.2^{+0.1}_{-0.2}$	~ 3.2‡	1.3(3)	−0.3(2)
Ogielski('85)[34]	MC sim. $8^3 \sim 64^3$	1.175(25)	2.9(3)	1.3(1)	−0.22(5)
Singh-Chakraverty('86)[30]	HTE up to w^{17}	1.2(1)	2.9(5)	1.3(2)	−0.25(17)

†) "MC" denotes Monte Carlo. "HTE" denotes the high-temperature expansion in $w \equiv \tanh^2(1/T)$.

‡) These $\gamma_{\rm s}$ are obtained from the scaling relation $\gamma_{\rm s} = (2-\eta)\nu$.

◇) These exponents are obtained on the assumption that $T_{\rm SG} \equiv 1.2$.

⋆) To know the definition of the exponents, see Appendix C.

the coherent-anomaly. Then a more efficient algorithm must be developed, because it comes now near the limit of the computational time.

Recent studies[29-30,32-34] concerning the spin-glass transition point and the critical exponents of the 3-dimensional $\pm J$ model with Ising spins are listed in Table 6.

After some oscillations between the positive conclusion and negative conclusions, some studies[30,32-34] on Monte-Carlo simulations of large scale concluded that the lower critical dimensionality is

$$2 \leq d_{\rm l} \leq 3, \tag{6.10}$$

i. e. the spin-glass transition occurs in the 3-dimensional Ising-spin-glass system. As shown in the last two rows of the Table 6, in 1986, the data[30] by the method of the high-temperature expansion, which seems to be quite independent of methods of simulations, agreed with the Monte-Carlo data[34] very well. Their conclusion is as follows:

$$T_{\rm SG}^{(*)} \simeq 1.2\ (J_0/k_{\rm B}), \tag{6.11}$$

and

$$\gamma_{\rm s} \simeq 2.9. \tag{6.12}$$

6.3 Summary

An effective-field theory was constructed and the results of the mean-field and Bethe approximations were re-derived. Further calculations and application of the CAM to them show usefulness of this theory. Especially for the 2-dimensional systems, we obtain the spin-glass transition point $T_{\rm SG}^{(*)} = 0$ and the critical exponent $\gamma_{\rm s}$ near $T_{\rm SG}^{(*)} = 0$, which agree with the results by other authors well, by calculations of rather small clusters. As for the 3-dimensional systems, however, we may have to treat larger clusters to evaluate accurate critical values by using the CAM theory.

Acknowledgments

I would like to express my gratitude to Professor Masuo Suzuki for his helpful discussions and suggestions. I am also grateful to Dr. Makoto Katori for his useful comments, Nobuyasu Ito for his kind advice on super computers, Showa Denko Scholarship for its financial support. This study is partially financed by the Research Fund of the Ministry of Education, Science and Culture.

A The Gauge Symmetry

The "gauge symmetry" property[13-14] of the Edwards-Anderson model was used in Section 2. In the present appendix, correlation functions which vanish in taking the quenched-averages of them, and "gauge-invariant" finite correlation functions are discussed.

Consider the Edwards-Anderson model with Ising spins; (2.1). The local "gauge transformation" of a state of a spin-configuration $\{\sigma_i\}$ and a bond-configuration $\{A_{ij}\}$, where $A_{ij} \equiv \text{sgn } J_{ij}$, is defined as follows:

$$\left\{ \begin{array}{ccccc} \sigma_i & \longrightarrow & \sigma_i' & \equiv & \tau_i \sigma_i, \\ A_{ij} & \longrightarrow & A_{ij}' & \equiv & \tau_i A_{ij} \tau_j, \end{array} \right. \tag{A.1}$$

where

$$\tau \equiv \pm 1. \tag{A.2}$$

The Hamiltonian with no magnetic fields $\mathcal{H}_0$ is invariant under this transformation:

$$\begin{aligned} \mathcal{H}_0\{\sigma_i, A_{ij}\} \equiv - \sum_{<ij>} |J_{ij}| \, \sigma_i A_{ij} \sigma_j \quad \longrightarrow \\ \mathcal{H}_0\{\sigma_i', A_{ij}'\} = - \sum_{<ij>} |J_{ij}| \, \sigma_i' A_{ij}' \sigma_j' \equiv \mathcal{H}_0\{\sigma_i, A_{ij}\}. \end{aligned} \tag{A.3}$$

The partition function of a given bond-configuration $\{A_{ij}\}$ is also invariant:

$$Z_0\{A_{ij}\} \equiv \mathrm{Tr}_\sigma\ e^{-\beta\mathcal{H}_0\{\sigma_i,A_{ij}\}} \longrightarrow$$
$$Z_0\{A'_{ij}\} = \mathrm{Tr}_{\sigma'}\ e^{-\beta\mathcal{H}_0\{\sigma'_i,A'_{ij}\}} \equiv Z_0\{A_{ij}\}. \tag{A.4}$$

In consequence, the set of all the bond-configurations are classified into "gauge-invariant" subsets, in which samples can be transformed to each other, and samples of the same subset have the same physical properties. In the following, two samples $\{A_{ij}\}$ and $\{A'_{ij}\}$ of the same gauge-invariant subset are denoted in the form

$$\{A_{ij}\} \sim \{A'_{ij}\}. \tag{A.5}$$

Owing to (A.4), we obtain for $\{A_{ij}\} \sim \{A'_{ij}\}$

$$\begin{aligned} F\{A_{ij}\} &\equiv -k_\mathrm{B}T\log Z_0\{A_{ij}\} \\ &= F\{A'_{ij}\}, \end{aligned} \tag{A.6}$$

$$\begin{aligned} \langle S\rangle_{\{A_{ij}\}} &\equiv \frac{1}{Z_0\{A_{ij}\}}\cdot \mathrm{Tr}\ S\{\sigma_i,A_{ij}\}\ e^{-\beta\mathcal{H}_0\{\sigma_i,A_{ij}\}} \\ &= \langle S\rangle_{\{A'_{ij}\}}, \end{aligned} \tag{A.7}$$

where S denotes such an operator as

$$S\{\sigma_i,A_{ij}\} = S\{\sigma'_i,A'_{ij}\}. \tag{A.8}$$

Each gauge-invariant subset can be characterized by the configuration of the frustrations $\{\Phi_{ijkl}\}$, where i, j, k, l are four sites around a plaquette and

$$\Phi_{ijkl} \equiv A_{ij}A_{jk}A_{kl}A_{li}\ : \tag{A.9}$$

See Figure 21. First, the configuration of the frustrations $\{\Phi_{ijkl}\}$ is gauge-invariant:

$$\Phi_{ijkl} \longrightarrow \Phi'_{ijkl} = A'_{ij}A'_{jk}A'_{kl}A'_{li} \equiv \Phi_{ijkl}. \tag{A.10}$$

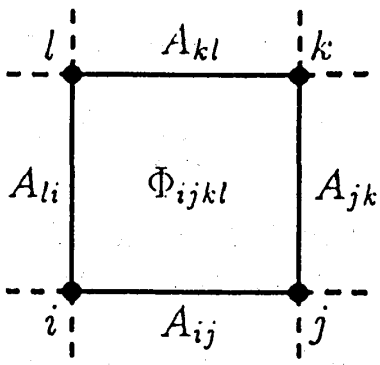

Figure 21: The definition of the frustration.

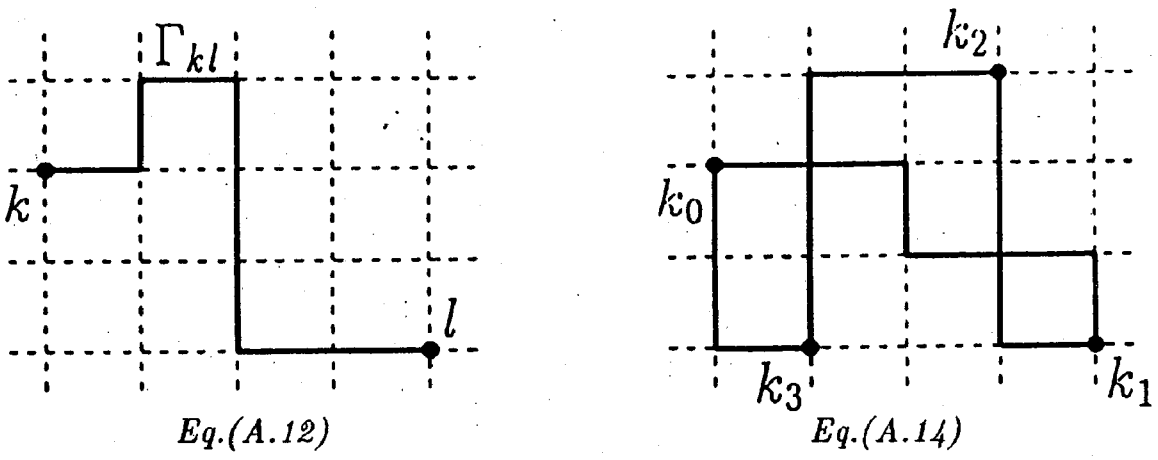

Figure 22: Gauge-invariant quantities.

Next, it is easily shown on small clusters that the partition function of the samples which belong to different gauge-invariant subsets are not equal to each other. Consequently, the gauge-invariant subset and the configuration of the frustrations have one-to-one correspondence. Quantities such as (A.6) and (A.7) can be written as functions of $\{\Phi_{ijkl}\}$.

Usual correlation functions are non-invariant:

$$\langle \sigma'_k \sigma'_l \rangle_{\{A'_{ij}\}} = \tau_k \tau_l \cdot \langle \sigma_k \sigma_l \rangle_{\{A_{ij}\}}. \tag{A.11}$$

The quenched averages of them with respect to a symmetric probability distribution vanish. The following quantities[14] are, however, gauge-invariant:

$$\begin{aligned} \langle \sigma'_k \cdot (\prod_{\Gamma_{kl}} A'_{ij}) \cdot \sigma'_l \rangle_{\{A'_{ij}\}} &= \langle \tau_k \sigma_k \cdot \tau_k (\prod_{\Gamma_{kl}} A_{ij}) \tau_l \cdot \tau_l \sigma_l \rangle_{\{A_{ij}\}} \\ &= \langle \sigma_k \cdot (\prod_{\Gamma_{kl}} A_{ij}) \cdot \sigma_l \rangle_{\{A_{ij}\}}, \end{aligned} \tag{A.12}$$

where Γ_{kl} denotes an arbitrary path of the bonds connecting the site k and the site l, and $\prod_{\Gamma_{kl}} A_{ij}$ denotes the product of all the A_{ij} accompanied by the bonds along the path Γ_{kl}: See Figure 22. Owing to the property

$$\prod_{\partial\Omega} A_{ij} = \prod_{<ijkl>\in\Omega} \Phi_{ijkl}, \tag{A.13}$$

it can be shown from (A.12) that such a product of correlation functions as follows is also gauge-invariant, i. e. a function of $\{\Phi_{ijkl}\}$:

$$\langle \sigma_{k_0} \sigma_{k_1} \rangle \langle \sigma_{k_1} \sigma_{k_2} \rangle \cdots \langle \sigma_{k_{n-2}} \sigma_{k_{n-1}} \rangle \langle \sigma_{k_{n-1}} \sigma_{k_0} \rangle; \tag{A.14}$$

see Figure 22. Especially, the squares of correlation functions

$$\langle \sigma_k \sigma_l \rangle^2 \tag{A.15}$$

are invariant; for example Equations (4.26) and (4.27).

On the other hand, with a symmetric probability distribution, quantities such as follows vanish:

$$[\langle \sigma_{k_0} \sigma_{k_1} \rangle \langle \sigma_{k_1} \sigma_{k_2} \rangle \cdots \langle \sigma_{k_{n-2}} \sigma_{k_{n-1}} \rangle \langle \sigma_{k_{n-1}} \sigma_{k_n} \rangle]_{\text{av.}} = 0 \quad \text{for } k_0 \neq k_n. \tag{A.16}$$

This property is used in the discussion below Equation (2.22).

B Decomposition Theorem

As Equation (4.32) in Section 4 , a simplification of calculations is possible. This simplification is essential to solve the Edwards-Anderson model on the Bethe lattice exactly in the paramagnetic phase. The following theorem 4 is mentioned in Suzuki's paper[10], but the proof of it is not very trivial.

Consider the two finite or infinite clusters Ω_A and Ω_B which contact with each other only at the articulation point j: See Figure 23. Some notations are defined as follows:

$$\mathcal{H}_A \equiv - \sum_{<ij> \in \Omega} J_{ij} \sigma_i \sigma_j, \tag{B.1}$$

$$\mathcal{H}_B \equiv - \sum_{<kl> \in \Omega} J_{kl} \sigma_k \sigma_l, \tag{B.2}$$

$$\mathcal{H}_{\text{tot}} \equiv \mathcal{H}_A + \mathcal{H}_B, \tag{B.3}$$

$$\langle \cdots \rangle_\alpha \equiv \frac{\text{Tr } \cdots e^{-\beta \mathcal{H}_\alpha}}{\text{Tr } e^{-\beta \mathcal{H}_\alpha}}, \tag{B.4}$$

where $\alpha =$ "tot", "A", "B".

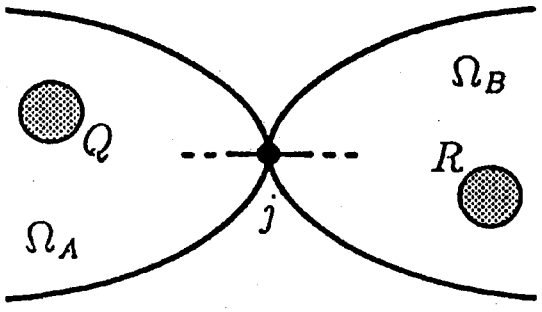

Figure 23: The two clusters Ω_A and Ω_B.

Theorem 1 *Consider an arbitrary Ising-spin system on the clusters defined above. Let Q and R be spin-operators on the clusters Ω_A and Ω_B correspondingly. The following identity holds:*

$$\langle QR\rangle_{\rm tot} = \frac{\langle Q\rangle_A\langle R\rangle_B + \langle Q\sigma_j\rangle_A\langle\sigma_j R\rangle_B}{1+\langle\sigma_j\rangle_A\langle\sigma_j\rangle_B}. \tag{B.5}$$

The proof: Let Tr_{-j} denote the trace with respect to all the spins except σ_j. The partition function of the total system can be written in the following form:

$$\begin{aligned} Z_{\rm tot} &\equiv \mathrm{Tr}\ e^{-\beta\mathcal{H}_{\rm tot}} \\ &= \sum_{\sigma_j=\pm1} (\mathrm{Tr}_{-j}\ e^{-\beta\mathcal{H}_A})(\mathrm{Tr}_{-j}\ e^{-\beta\mathcal{H}_B}). \end{aligned} \tag{B.6}$$

In the case of $\sigma_j = \pm 1$ correspondingly,

$$\begin{aligned} (\mathrm{Tr}_{-j}\ e^{-\beta\mathcal{H}_A})(\mathrm{Tr}_{-j}\ e^{-\beta\mathcal{H}_B}) &= (\mathrm{Tr}\ \frac{1\pm\sigma_j}{2}e^{-\beta\mathcal{H}_A})(\mathrm{Tr}\ \frac{1\pm\sigma_j}{2}e^{-\beta\mathcal{H}_B}) \\ &= Z_A Z_B \cdot \frac{1\pm\langle\sigma_j\rangle_A}{2}\cdot\frac{1\pm\langle\sigma_j\rangle_B}{2}, \end{aligned} \tag{B.7}$$

where

$$Z_\alpha \equiv \mathrm{Tr}\ e^{-\beta\mathcal{H}_\alpha} \quad \text{for } \alpha = A,\ B. \tag{B.8}$$

The operators $\dfrac{1\pm\sigma_j}{2}$ in Equation (B.7) pick up only the case $\sigma = \pm 1$ correspondingly. Substitution (B.7) in (B.6) yields

$$Z_{\rm tot} = \frac{Z_A Z_B}{2}(1+\langle\sigma_j\rangle_A\langle\sigma_j\rangle_B). \tag{B.9}$$

The similar calculation gives

$$\begin{aligned} \langle QR\rangle^{\rm u}_{\rm tot} &\equiv \sum_{\sigma_j=\pm1} (\mathrm{Tr}_{-j}\ Q\ e^{-\beta\mathcal{H}_A})(\mathrm{Tr}_{-j}\ R\ e^{-\beta\mathcal{H}_B}) \\ &= \frac{Z_A Z_B}{2}(\langle Q\rangle_A\langle R\rangle_B + \langle Q\sigma_j\rangle_A\langle\sigma_j R\rangle_B). \end{aligned} \tag{B.10}$$

From Equations (B.9) and (B.10), we obtain

$$\langle QR\rangle_{\rm tot} \equiv \frac{\langle QR\rangle^u_{\rm tot}}{Z_{\rm tot}} \tag{B.11}$$

in the form (B.5). Q.E.D.

Lemma 2 *Consider a spin operator S of an arbitrary Ising spin-glass system, which satisfies the condition that the inequality $|\langle S\rangle| \le 1$ holds for all the bond-configurations at a temperature.*

1. It holds at that temperature that

$$[\langle S\rangle^2]_{\text{av.}} = 0 \quad \Longrightarrow \quad [\langle S\rangle^n]_{\text{av.}} = 0 \quad \textit{for } {}^\forall n \geq 2. \tag{B.12}$$

2. Especially, it holds at an arbitrary temperature that

$$[\langle \sigma\rangle^2]_{\text{av.}} = 0 \quad \Longrightarrow \quad [\langle \sigma\rangle^n]_{\text{av.}} = 0 \quad \textit{for } {}^\forall n \geq 2. \tag{B.13}$$

The proof: The condition $|\langle S\rangle| \leq 1$ gives

$$|\langle S\rangle^n| \leq \langle S\rangle^2 \quad \text{for } {}^\forall n \geq 2. \tag{B.14}$$

Taking the quenched-averages of it yields

$$|\,[\langle S\rangle^n]_{\text{av.}}| \leq [\,|\langle S\rangle^n|\,]_{\text{av.}} \leq [\langle S\rangle^2]_{\text{av.}} = 0. \tag{B.15}$$

Q.E.D.

Lemma 3 *Consider a spin operator S and a real non-singular function f of an arbitrary Ising spin-glass system.*

1. It holds that

$$[\langle S\rangle^2]_{\text{av.}} = 0 \quad \Longrightarrow \quad [\langle S\rangle \cdot f]_{\text{av.}} = 0. \tag{B.16}$$

2. In the case that the operator S satisfies the condition that the inequality $|\langle S\rangle| \leq 1$ holds for all the bond-configurations at a temperature, it holds at that temperature that

$$[\langle S\rangle^2]_{\text{av.}} = 0 \quad \Longrightarrow \quad [\langle S\rangle^n \cdot f]_{\text{av.}} = 0 \quad \textit{for } {}^\forall n \geq 1. \tag{B.17}$$

The proof: From Cauchy-Schwarz's inequality, we obtain

$$[\langle S\rangle^n \cdot f]^2_{\text{av.}} \leq [\langle S\rangle^{2n}]_{\text{av.}} \cdot [f^2]_{\text{av.}}. \tag{B.18}$$

1. For $n = 1$, it gives

$$[\langle S\rangle \cdot f]^2_{\text{av.}} \leq [\langle S\rangle^2]_{\text{av.}} \cdot [f^2]_{\text{av.}} = 0. \tag{B.19}$$

2. Besides, for the operator S which satisfies the condition mentioned above, Lemma 2 yields

$$[\langle S\rangle^n \cdot f]^2_{\text{av.}} \leq [\langle S\rangle^{2n}]_{\text{av.}} \cdot [f^2]_{\text{av.}} = 0 \quad \text{for } {}^\forall n \geq 1. \tag{B.20}$$

Q.E.D.

Theorem 4 (Decomposition Theorem) *Consider the spin operators Q and R of the Ising spin-glass system on the previously defined clusters Ω_A and Ω_B correspondingly.*

1. *At a finite temperature, it holds that*

$$[\langle Q\rangle_A^2]_{\rm av.} = [\langle R\rangle_B^2]_{\rm av.} = [\langle\sigma_j\rangle_A^2]_{\rm av.} = [\langle\sigma_j\rangle_A^2]_{\rm av.} = 0 \quad \Longrightarrow$$
$$\begin{cases} [\langle QR\rangle_{\rm tot}]_{\rm av.} &= [\langle Q\sigma_j\rangle_A]_{\rm av.}[\langle\sigma_j R\rangle_B]_{\rm av.}, \\ [\langle QR\rangle_{\rm tot}^2]_{\rm av.} &= [\langle Q\sigma_j\rangle_A^2]_{\rm av.}[\langle\sigma_j R\rangle_B^2]_{\rm av.}. \end{cases} \tag{B.21}$$

2. *In the case that the operators Q and R satisfy the condition that the inequalities $|\langle Q\rangle| \le 1$, and $|\langle R\rangle| \le 1$ hold at a temperature for all the bond-configurations, it holds at that temperature that*

$$[\langle Q\rangle_A^2]_{\rm av.} = [\langle R\rangle_B^2]_{\rm av.} = [\langle\sigma_j\rangle_A^2]_{\rm av.} = [\langle\sigma_j\rangle_A^2]_{\rm av.} = 0 \quad \Longrightarrow$$
$$[\langle QR\rangle_{\rm tot}^n]_{\rm av.} = [\langle Q\sigma_j\rangle_A^n]_{\rm av.}[\langle\sigma_j R\rangle_B^n]_{\rm av.} \quad \textit{for } {}^\forall n \in N. \tag{B.22}$$

The proof: At finite temperatures, we can set for all the bond-configurations

$$|\langle\sigma_j\rangle_A| < 1, \text{ and } |\langle\sigma_j\rangle_B| < 1. \tag{B.23}$$

Therefore the expansion of Equation (B.5)

$$\begin{aligned} \langle QR\rangle_{\rm tot} &= \frac{\langle Q\rangle_A\langle R\rangle_B + \langle Q\sigma_j\rangle_A\langle\sigma_j R\rangle_B}{1 + \langle\sigma_j\rangle_A\langle\sigma_j\rangle_B} \\ &= \{\langle Q\rangle_A\langle R\rangle_B + \langle Q\sigma_j\rangle_A\langle\sigma_j R\rangle_B\} \\ &\quad \times\{1 + \sum_{k=1}^{\infty}(-1)^k\langle\sigma_j\rangle_A^k\langle\sigma_j\rangle_B^k\} \end{aligned} \tag{B.24}$$

converges absolutely. This expansion yields for ${}^\forall n \in N$

$$\begin{aligned} [\langle QR\rangle_{\rm tot}^n]_{\rm av.} &= \Bigg[\sum_{l=0}^{n}\sum_{m=0}^{n}\langle Q\rangle_A^l\langle R\rangle_B^l\langle Q\sigma_j\rangle_A^{n-l}\langle\sigma_j R\rangle_B^{n-l} \\ &\quad \times\{\sum_{k=1}^{\infty}(-1)^k\langle\sigma_j\rangle_A^k\langle\sigma_j\rangle_B^k\}^m\Bigg]_{\rm av.}. \end{aligned} \tag{B.25}$$

1. In the case of $n = 1$ or 2, the terms $l = 1$ or $m = 1$, 2 of Equation (B.25) vanish owing to Lemma 3. The term that $l = 2$ and $m = 0$ vanishes because of

$$[\langle Q\rangle_A^2\langle R\rangle_B^2]_{\rm av.} = [\langle Q\rangle_A^2]_{\rm av.}[\langle R\rangle_B^2]_{\rm av.} = 0. \tag{B.26}$$

The remaining term gives (B.21).

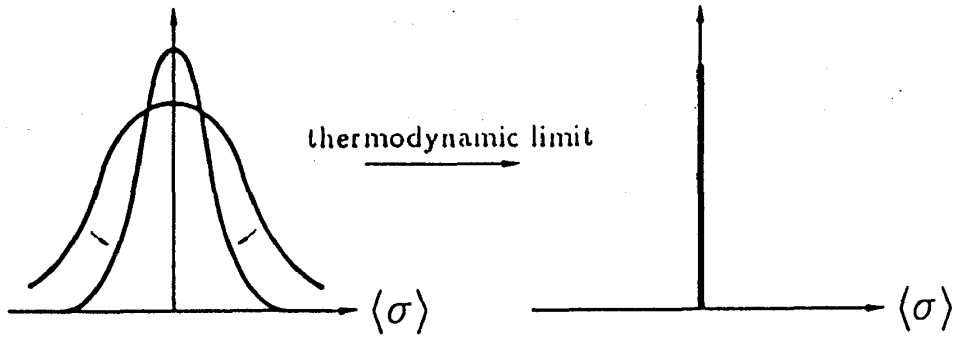

Figure 24: The fraction of the samples of $\langle\sigma\rangle \neq 0$ in the paramagnetic phase.

2. Besides, for the operators Q and R which satisfy the condition mentioned above, all the terms $l \geq 1$ or $m \geq 1$ vanish for $^{\forall}n \in N$ owing to Lemma 3, and Equation (B.22) holds.

Q.E.D.

Though the ferromagnetic transition may occur on some samples even in the paramagnetic phase, it seems that Theorem 4 can be derived from Theorem 1 formally on the assumption of $\langle\sigma\rangle = 0$. This observation suggests that the fraction of the samples of $\langle\sigma\rangle \neq 0$ is vanishing in the thermodynamic limit: See Figure 24.

C Some Definitions of Critical Exponents

The definitions[2] of the exponent η,γ and ν are listed here. The exponent η is defined as follows:

$$[\langle\sigma_i\sigma_j\rangle^2]_{\text{av.}} \propto \frac{e^{-r_{ij}/\xi_{\text{EA}}}}{r_{ij}^{d-2+\eta}} \quad \text{as} \quad r_{ij} \to \infty. \tag{C.1}$$

The exponent γ_s is defined as follows:

$$\chi_{\text{EA}} \equiv \frac{1}{N} \cdot \sum_{i,j} [\langle\sigma_i\sigma_j\rangle^2]_{\text{av.}} \propto \frac{1}{(T - T_{\text{SG}})^{\gamma_s}} \quad \text{as} \quad T \to T_{\text{SG}} + 0. \tag{C.2}$$

The exponent ν is defined by the behaviour of ξ_{EA} appearing in (C.1) as follows:

$$\xi_{\text{EA}} \propto \frac{1}{(T - T_{\text{SG}})^{\nu}} \quad \text{as} \quad T \to T_{\text{SG}} + 0. \tag{C.3}$$

The following scaling-relation holds:

$$\gamma_s = (2 - \eta)\nu. \tag{C.4}$$

References

[1] S. F. Edwards & P. W. Anderson: *J. Phys. F***5** (1975) 965.

[2] for a review, K. Binder & A. P. Young: *Rev. Mod. Phys.* **58** (1986) 801.

[3] D. Sherrington & S. Kirkpatrick: *Phys. Rev. Lett.* **35** (1975) 1972.

[4] G. Parisi: *Phys. Rev. Lett.* **43** (1979) 1754; *J. Phys. A***13** (1980) L115, 1101, 1887; *Phys. Rep.* **67** (1980) 97.

[5] J. H. Chen & T. C. Lubensky: *Phys. Rev. B***16** (1977) 2106.

[6] M. Suzuki: *J. Phys. Soc. Jpn.* **55** (1986) 4205.

[7] M. Suzuki, M. Katori, & X. Hu: *J. Phys. Soc. Jpn.* **56** (1987) 3092.

[8] M. Katori, & M. Suzuki: *J. Phys. Soc. Jpn.* **56** (1987) 3113.

[9] S. Katsura, S. Inawashiro, & S.Fujiki: *Physica A***99** (1979) 193.

[10] M. Suzuki: *J. Phys. Soc. Jpn.* **57** (1988) 2310; *J. de Phys. Colloque C***8** (1988) 1519.

[11] M. Suzuki: Recent Progress in Many-Body Theories, to be published by Plenum Pub. co., ed. by Y. Avishai.

[12] N. Kawashima & M. Suzuki: *J. Phys. Soc. Jpn.* **58** (1989) 3123.

[13] G. Toulouse: *Commun. Phys.* **2** (1977) 115.

[14] E. Fradkin & B. A. Huberman & S. H. Shenker: *Phys. Rev. B***18** (1978) 4789.

[15] F. Matsubara & M. Sakata: *Prog. Theor. Phys.* **55** (1976) 672

[16] S. Katsura & S. Fujiki: *J. Phys. C***12** (1979) 1087.

[17] S. Katsura: *Prog. Theor. Phys. Supplement* **87** (1986) 139; Errata, *Prog. Theor. Phys.* **79** (1988) 251.

[18] M. Sasaki & S. Katsura: *Physica A***157** (1989) 1195.

[19] C. Kwon & D. J. Thouless: *Phys. Rev. B***37** (1988) 7649

[20] S. Katsura: *Prog. Theor. Phys.* **55** (1976) 1049.

[21] S. Fujiki & S. Katsura: *Prog. Theor. Phys.* **65** (1981) 1130.

[22] M. E. Fisher & M. N. Barber: *Phys. Rev. Lett.* **28** (1972) 1516.

[23] I. Morgenstern & K. Binder: *Phys. Rev. Lett.* **43** (1979) 1615; *Phys. Rev. B***22** (1980) 288.

[24] I. Morgenstern: *Phys. Rev. B***25** (1982) 6071.

[25] K. Binder: *Z. Phys. B***48** (1982) 319.

[26] A. P. Young: *Phys. Rev. Lett.* **50** (1983) 917.

[27] W. L. McMillan: *Phys. Rev. B***28** (1983) 5216.

[28] H. F. Cheung & W. L. McMillan: *J. Phys. C***16** (1983) 7027.

[29] A. P. Young: *J. Phys. C***18** (1984) L517.

[30] R. R. P. Singh & S. Chakravarty: *Phys. Rev. Lett.* **57** (1986) 245; *Phys. Rev. B***36** (1987) 546, 559.

[31] R. N. Bhatt & A. P. Young: *Phys. Rev. B***37** (1988) 5606.

[32] A. T. Ogielski & I. Morgenstern: *Phys. Rev. Lett.* **54** (1985) 928; *J. Appl. Phys.* **57** (1985) 3382.

[33] R. N. Bhatt & A. P. Young: *Phys. Rev. Lett.* **54** (1985) 924.

[34] A. T. Ogielski: *Phys. Rev. B***32** (1985) 7384.